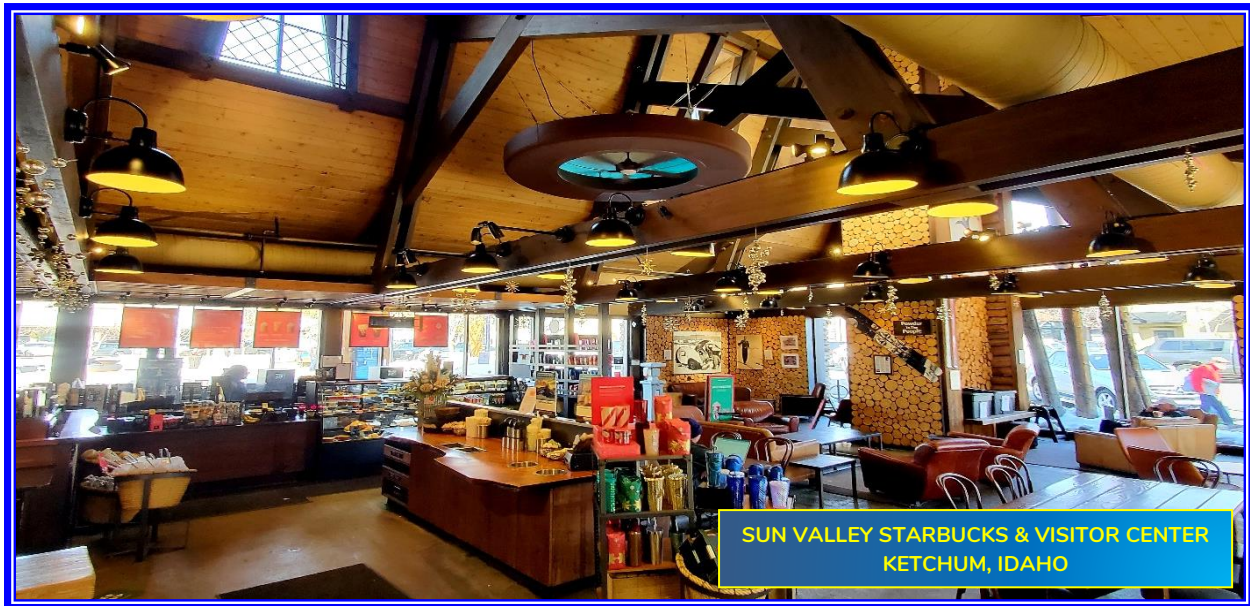


# PREVENTING RESPIRATORY INFECTIONS:

## A unified dose model and IAQ risk assessment tool



by Anu Sood, PE, CPP  
Founder and CEO



LUV Systems, Inc.  
EPC Western Plaza  
18726 South Western Avenue #407  
Gardena, CA 90248  
[LuvSystems.com](http://LuvSystems.com)  
844-THE-HALO (844-843-4256)



Issue Date: **February 22, 2022**

**CONFIDENTIAL/TRADE SECRET:** The information contained herein is considered business confidential and trade secret, exclusively for evaluation purposes by the intended recipient, and should only be shared with third parties on a need-to-know basis in context and in accordance with express written authorization from LUV Systems, Inc.

**TRANSPARENCY NOTICE:** This document and supporting research are wholly funded by LUV Systems, Inc., which is presently designing low-UVC consumer and commercial disinfection products. If there is any concern that this could be a potential financial or other conflict-of-interest, please be assured that our primary objective in these efforts is to develop and introduce safe, effective, and reliable disinfection products to the marketplace.

Literature citations and internet links are current as of the issue date on this cover page. **the halō** is not a medical device and LUV Systems, Inc. makes no medical claims. All pictures are shown for illustration purposes only, and actual products may vary. **the halō** is covered by various pending patents.

© 2023 LUV Systems, Inc. All rights reserved.

230116

## Abstract

The COVID-19 pandemic has demonstrated an urgency to understand how respiratory infections spread within indoor spaces, and to develop infection risk assessment tools to guide public health policy makers, regulators, and facility management. Such tools are critically needed, as there is no established health risk-based IAQ regulatory standard for pathogen exposure in public, non-health care areas. While environmental agencies regulate excess cancer risk to below 100 in one million over 70 years, in just two years the United States has already seen close to 3,000 pandemic deaths and over 240,000 infections per million population.

Respiratory transmission is airborne by definition, and occurs almost exclusively indoors. This paper characterizes the dynamics and processes of indoor generation, transport, and fate of respiratory pathogens through infection, and reviews the functional performance of mitigation strategies, based on a proposed unified indoor air infectious dose model and IAQ risk assessment tool. The model addresses two critical elements of the respiratory infection cycle that are consistently underrepresented or ignored by researchers as documented in relevant literature:

- The breathing zone where pathogens and respiratory infections are generated; and,
- Respiratory jets that create localized nonhomogeneous airborne pathogen loadings in the proximity of infected persons.

Well-mixed models do not adequately consider localized pathogen loadings, such as proximal to or downwind exposures, and thereby underestimate infection risk by >20x. This model demonstrates the best approach to mitigate risk is to control potentially infectious breathing zone air via directed airflow to disperse respiratory jets upward and minimize mixing of treated and untreated air.

The unified infectious dose model predicts and quantifies benefits and limitations of respiratory infection mitigation measures. The model may serve as a useful tool for IAQ risk assessment and to guide mitigation strategies and public health policy. Predictions are within 13% of the CDC's 15-min guidance for close contact and potential COVID-19 exposure. Boundary conditions and consolidated source/sink terms are incorporated in the model's underlying equation:

$$N(t) = N_0 e^{-\beta t} + (\alpha/\beta)(1 - e^{-\beta t})$$

where  $N(t)$  is the airborne pathogen loading at time  $t$ ,  $N_0$  is the initial pathogen loading at  $t = 0$ ,  $\alpha$  is the generation coefficient for pathogen discharge into the air via human shedding mechanisms, and  $\beta$  is the depletion coefficient for pathogen attenuation by ventilation, treatment, filtration, and natural decay.  $\alpha$  and  $\beta$  incorporate multiple zone factors to represent localized, nonhomogeneous conditions for each dynamic mechanism.  $N(t)$  is proportional to the pathogen uptake rate and probability of a new infection based on the defined infectious dose for SARS-CoV-2 or other respiratory pathogen.

Masks, partitions, and social distancing are found to be reasonably effective strategies for short-term exposures under 1 hr, as respiratory jets are dispersed away from the breathing zone. For long-term exposures > 1 hr, breathing zone control, directed airflow, and effective treatment and/or filtration are critical. A simple upflow ceiling fan can provide limited reduction of short-term infection risk, especially for proximal or downwind receptors.

There is currently no established and actionable health-based IAQ metric for respiratory infections. An Airborne Pathogen Mitigation Index (APMI) is proposed, correlated with exposure time. APMI results are mostly consistent with the less versatile risk parameter recently proposed by Peng (2022), despite 30x variation in infectious pathogen quanta generation rates.<sup>1</sup>

A new product - **the halō**, incorporating an upflow fan with an encapsulated low-wavelength germicidal UVC light ring, is evaluated with the model and shown to be quantitatively better than any other strategy to mitigate short- and long-term respiratory infection risk. With a continuous source actively shedding pathogens, **the halō** is 10x better than any air disinfection option (including HVAC-based treatment/filtration or ventilation) and 3x better than social distancing with masks. With no source and pre-existing airborne pathogen loading, **the halō** clears the air >2x faster than any other option.

**the halō** provides over 30 equivalent air changes/hour (ACH<sub>e</sub>) for a 1,000 ft<sup>2</sup> room, over twice the CDC standard for critical health care facilities, by treating 20% of a room's air every minute with effective breathing zone control and directional airflow.<sup>2</sup> HVAC-based disinfection/filtration, increasing ventilation, portable air purifiers, and other available disinfection products may increase ACH<sub>e</sub>, yet are categorically ineffective as they do not disperse respiratory jets, control the breathing zone, and prevent mixing of treated and untreated air. Ventilation strategies, specifically implemented to increase the clean air delivery rate, significantly increase utility costs, HVAC retrofit and maintenance needs, and contribute to excess CO<sub>2</sub> emissions.



<sup>1</sup> <https://pubs.acs.org/doi/10.1021/acs.est.1c06531?ref=pdf>

<sup>2</sup> For more on directional airflow, see <https://www.cdc.gov/coronavirus/2019-ncov/community/ventilation.html#considerations>

## About the author

**Anu Sood, PE, CPP**  
**Founder & CEO, LUV Systems, Inc.**

Anu is a California-registered Professional Chemical Engineer with over 35 years of air quality and environmental engineering experience. Recognized for cost-effective solutions for government and corporate environmental stewardship, he has led and implemented multimedia studies including:

- Contaminant and pathogen transport and fate dynamics
- Criteria and toxic air emissions characterization
- Human and ecological health risk assessment
- IAQ surveys and enhancement strategies
- Multi-stage physical, chemical, and biological treatment processes
- Complex non-equilibrium systems modeling
- Best Available Control Technology determinations
- Optimal pollutant capture and control system design
- Effects of ionizing energy and particles on biological tissue and pathogens in environmental media
- Regional clean air and health-risk mitigation strategies
- Illness/endpoint dose-response toxicology.



Clients have included the U.S. Departments of Defense and Energy, Amtrak, City and County of Los Angeles, school districts, airports, hospitals, property managers, public works facilities, and varied industrial manufacturers. Anu has bachelor's and master's degrees in chemical engineering and chemical engineering practice from MIT, and he is a first-round [Certified Permitting Professional](#) with the South Coast Air Quality Management District.

## Acknowledgements

The author acknowledges extensive technical and editorial contributions by the LUV Systems team, including VP Engineering Danish Khatri, General Counsel Sandeep Seth, and Compliance Manager Stanley Thompson. Dr. Kevin Hickerson of The Earthineering Company is noted for his critical peer review efforts. MIT Chemical Engineering Professor Alan Hatton is appreciated for his inspirational words, along with the research contributions of Boston University Medical School and Professor Anthony Griffiths'



group. Other LUV Systems team members, partners, collaborators, and consultants including Neeraj Chaudhary, are recognized for their support over the past two years as this paper and underlying theory have come to fruition, a practical indoor air modeling and infection risk assessment tool has been developed, and the **halō** air disinfection system has officially launched.



## Table of Contents



Abstract.....	<a href="#">.ii</a>
About the Author .....	<a href="#">.iii</a>
Acknowledgements .....	<a href="#">.iii</a>
Revision Log .....	<a href="#">.vi</a>
Acronyms and Symbols Used.....	<a href="#">(pending)</a>
1 Introduction: Respiratory Infections .....	<a href="#">1</a>
2 Unified Indoor Air Infectious Dose Model .....	<a href="#">3</a>
2.1 Rationale	
2.2 Literature Review	
2.3 The Fundamental Pathogen Material Balance	
2.4 Pathogen Generation ( $N_G$ )	
2.5 Pathogen Transport ( $N_S$ , $N_R$ )	
2.6 Pathogen Fate ( $N_E$ , $N_T$ , $N_F$ , $N_D$ , $N_I$ )	
2.6.1 Atmospheric Ventilation	
2.6.2 Treatment, Filtration	
2.6.3 Natural Decay	
2.6.4 Inhalation and the Respiratory Jet	
2.6.5 Evaporation of Moisture	
2.6.6 Heat Dissipation and Thermal Buoyancy	
2.6.7 Mass Diffusion	
2.6.8 Momentum Transfer	
2.6.9 The Inhalation Equation	
2.6.10 Face Coverings, Partitions	
2.7 Unified Infectious Dose Model ( $N(t)$ , $\alpha$ , $\beta$ , $U_{PPQ}$ , $U_{INF}$ , $t_{INF}$ )	
2.8 Base Case & Assumptions	
2.8.1 Model Configuration	
2.8.2 Generation	
2.8.3 Depletion, Reentrainment	
2.8.4 Ventilation, Treatment, Filtration	
2.8.5 Inhalation	

2.8.6	Proximity, Downwind Parameters	
2.8.7	Consolidated Generation/Depletion Coefficients	
2.8.8	Infectious Dose Parameters	
2.9	Model Uncertainty, Calibration, Development	
<b>3</b>	<b>Assessment of Mitigation Strategies .....</b>	<b>20</b>
3.1	Social Distancing, Masks, Partitions	
3.2	Ventilation and Central HVAC	
3.3	Portable Air Purifiers	
3.4	Ceiling-Based Systems (Troffers, Upper-Room UVGI, Ceiling Fans)	
3.5	<b>the halō</b> : A Viable Alternative (Encapsulated Low-UVC Active Disinfection)	
3.6	Entering an Infectious Space (No Continuous Source)	
3.7	Comparison to ACH and CADR	
3.8	Airborne Pathogen Mitigation Index (APMI)	
<b>4</b>	<b>the halō - Air Disinfection with Breathing Zone Control .....</b>	<b>29</b>
4.1	Airflow	
4.2	Encapsulated Low-UVC Active Disinfection	
4.3	Microorganism Susceptibility Factor to Low-UVC	
4.4	Minimize Mixing of Treated and Untreated Air	
4.5	Impact on HVAC Systems	
4.6	Comparative Energy Burden and Carbon Footprint	
<b>5</b>	<b>Conclusions .....</b>	<b>34</b>
<b>6</b>	<b>References .....</b>	<b>(pending)</b>

## Tables

- 1 Average respiratory jet velocity and propagation distance
- 2 List of input terms and nomenclature for the unified infectious dose model
- 3 Model parameters,  $\alpha/\beta + t_{INF}$  results for alternative scenarios (ascending  $t_{INF}$ )
- 4 Alternative model parameters (initial PPQ load, no continuing source, ascending  $\beta$ /descending  $T_{50}$ )
- 5 Comparison of  $ACH_e$ ,  $\beta$ , and APMI
- 6 APMI and risk parameter ( $H$ , pp  $h^2 m^{-3}$ ) from Peng (2022)
- 7 Summary of low-UVC inactivation studies with RNA/DNA virions
- 8 Energy burden and carbon footprint at 2.8 and 12 ACH (annualized per classroom; excludes capital costs; rounded)

## Figures

- 1 Base case (no mitigation) infectious dose model results
- 2 Model results for masks, social distancing, partitions
- 3 HVAC mixes breathing zone air and spreads pathogens throughout the room
- 4 Model results for ventilation and HVAC+treatment
- 5 Model results for Honeywell HPA300 portable air purifier x2
- 6 Model results for troffers, upper-room UVGI, ceiling fans
- 7 Model results for the halō Model 5R/M and comparison
- 8 Model results with no continuing source
- 9  $ACH_e$  for ventilation, treatment, and filtration strategies
- 10 APMI for considered mitigation approaches (continuous source)
- 11 Expanded view of the halō
- 12 Upflow fan airflow patterns (before modulation)
- 13 Low-UVC dose needed for 99.9% virus inactivation (semilog)



Date	Revision #	Summary of Changes
16 Dec 2021	0	<ul style="list-style-type: none"> <li>First release.</li> </ul>
22 Feb 2022	1	<ul style="list-style-type: none"> <li>Introduce Airborne Pathogen Mitigation Index (APMI).</li> <li>Incorporate comparison to Peng (2022).</li> <li>Add paragraph comparing the amount of indoor air we breathe relative to food and liquids.</li> <li>Add paragraph on mask efficiencies.</li> <li>Add references and discussion on excess cancer risk (SCAQMD etc.).</li> <li>Add reference on "invisible air bridges."</li> <li>Explain "reasonable worst-case" basis.</li> <li>Add explanation of variable shedding rate for variants and other pathogens.</li> <li>Clarify theoretical relation between <math>f_{M,v}</math> and <math>f_{M,g}</math>.</li> <li>Add discussion of N95 masks and health-care workers.</li> <li>Add discussion on ceiling fans upflow/downflow without treatment.</li> <li>Add APMI comparison to Table 5.</li> <li>Add APMI section and new Figure 10, and new Table 6.</li> <li>Clarify first-order susceptibility factor assumption.</li> <li>Add discussion of <math>ACH_{le}</math>.</li> <li>Update abstract and conclusions accordingly.</li> <li>Update images with blue glow versions, added a few.</li> <li>Editorial corrections including new revision log section.</li> </ul>

## 1 Introduction: Respiratory Infections [\[back to TOC\]](#)

Respiratory transmission occurs when an uninfected individual breathes in sufficient infectious air exhaled by others in buildings and indoor spaces. Respiratory infections are caused by germs in the infectious air, such as viruses and bacteria, which spread by respiratory fluids including small droplets (aerosols). Airborne transmission is documented<sup>3,4</sup> for viral and bacterial pathogens including all known coronaviruses and influenza/flu, rhinoviruses (common cold),<sup>5</sup> tuberculosis (including drug-resistant strains),<sup>6</sup> Legionnaires' disease, measles, and viral pneumonia. The COVID-19 pandemic has propagated relentlessly through many countries and jurisdictions, with policy makers offering inconsistent and seemingly arbitrary, knee-jerk directives while societies struggle with widespread illness and premature deaths, overburdened healthcare systems, debate over the pros and cons of draconian masking and social distancing policy, and impose a patchwork of regional lockdowns and travel restrictions.<sup>7</sup> The global response has been hampered by a lack of clear scientific understanding of how respiratory infections are transmitted; inadequate risk assessment tools to quantify actionable infection risk; and frequently non-existent regulatory authority and standards to mitigate indoor air infection risk – including national, regional, and local health, environmental, and public welfare agencies.



For people to continue their indoor lives unfettered and without fear of respiratory infection, two essential and unique *in situ* (while people are present) processes must be implemented for indoor public spaces, without fostering cross-infection, and with the highest standards for efficacy and safety:<sup>8</sup>

1. **Ventilation** - Active removal of potentially infectious air from the breathing zone (directional airflow) as quickly as possible wherever pathogens are generated, irrespective of supplemental measures including social-distancing and masks.
2. **Disinfection** - Removal or inactivation of pathogens in any air that is returned to the breathing zone.

**Effective disinfection without ventilation** (where people are breathing, without actively moving the air) is inherently unsafe – methods used to disinfect biological pathogens naturally have adverse physical impacts on human cells, as well as exposed materials and surfaces. **Effective ventilation with no disinfection** requires all the air to be replaced continuously by fresh air, and this is impractical and resource intensive.



In conjunction with baseline ventilation, which is always necessary to remove carbon dioxide and refresh the indoor air in occupied locations, *in situ* air disinfection methods include dispersion of chemicals or energy in the room volume to inactivate pathogens. Examples include oxidizers such as hydroxyl ions or ozone, ultraviolet light, radiofrequency waves, and ultrasonic energy. The only way to use any of these agents safely is to provide adequate containment and prevent broad dispersal of the agent – a clear challenge when the objective is to continuously disinfect the entire breathing zone of a room.

<sup>3</sup> <https://epi.dph.ncdhhs.gov/cd/diseases/respiratory.html>

<sup>4</sup> <https://www.cdc.gov/coronavirus/2019-ncov/science/science-briefs/sars-cov-2-transmission.html>

<sup>5</sup> <https://www.aappublications.org/content/35/1/1.2>

<sup>6</sup> <https://www.cdc.gov/tb/topic/drtb/default.htm>

<sup>7</sup> <https://www.cnn.com/2021/12/05/health/covid-pandemic-global-solutions-toolkit-cmd-intl/index.html>

<sup>8</sup> The fundamental approach of air pollution engineering is to capture pollutants (ventilation) and then control them (disinfection) via physical, chemical, and/or thermal (energy) processes. Capture and control have the two distinct efficiencies that independently contribute to overall system effectiveness.



For respiratory pathogens such as SARS-CoV-2, air disinfection strategies focus on clean air delivery rate (CADR) and equivalent air change rate per hour (ACH<sub>e</sub>) – although simply increasing ventilation or using portable air purifiers does not reduce the short-term exposure risk due to localized airborne pathogen concentrations. Exposure to localized airborne pathogen loadings can be mitigated with effective dispersal of respiratory jets, control of the breathing zone, and directional airflow. Furthermore, increased ventilation ACH results in much greater energy use, higher equipment modification and maintenance costs, and excess CO<sub>2</sub> emissions.

This paper offers a practical and unified indoor air infectious dose model<sup>9</sup> to address multiple concurrent processes within respiratory transmission, incorporating airflow and aerosol dynamics coupled with a broad range of respiratory infection mitigation measures to:

- Answer the question, “How safe is your air?”
- Provide a critical review of transmission risk mitigation strategies including indoor air disinfection methods;
- Propose a new health-based IAQ metric for respiratory infections, the Airborne Pathogen Mitigation Index (APMI), as an indoor air risk parameter correlated with exposure time; and,
- Introduce a novel approach combining active ventilation and disinfection processes wherever people are present, consistent with established health standards and best practices, and concurrently achieving effectiveness and safety with a upflow ceiling fan to control and direct breathing zone air into an encapsulated low-wavelength germicidal UVC light ring – providing a remarkable ACH<sub>e</sub> rate > 30:



the halō™  
the halō by LUV Systems

<sup>9</sup> This comparative analysis is with discrete values for critical parameters such as shedding rate, infective dose, mask efficacy, etc. – attempting to represent median, (50<sup>th</sup> percentile values for each broad-ranging variable. The model inherently allows for distribution function inputs for these variables, providing for probabilistic results including event thresholds such as worst, maximum reasonable worst, and most likely infection risk determination.



## 2 Unified Indoor Air Infectious Dose Model [\[back to TOC\]](#)

### 2.1 Rationale [\[back to TOC\]](#)

The average person breathes in over 10,000 L of predominantly indoor air per day. This is > 25 lb/day, more than we eat and drink combined every day on weight and volume bases. While there are extensive and rigorous health-based laws and standards to ensure our food and water supplies are safe to eat and drink (as well as outdoor air), there are no meaningful criteria for defining, predicting, or assessing the potential health risks associated with breathing indoor air laden with potential respiratory pathogens.

Globally, indoor spaces are woefully inadequate at preventing airborne transmission of pathogens between people. Various strategies have been practiced, including social distancing and occupancy constraints, face coverings (masks), transparent partitions between people, HVAC retrofits and increased dilution with outside air, portable air purifiers, and upper room air disinfection systems such as ceiling fans and troffers. Yet, two years into the COVID-19 pandemic, policy makers continue to offer inconsistent, reactive, and seemingly arbitrary control measures, compounded by:

- Lack of clear scientific understanding of primary respiratory infection transmission mechanisms;
- Perpetual uncertainty about emerging COVID-19 variants and the “next wave,” in the context of seesaw governmental directives requiring various combination of masks, mandatory worker/student/visitor vaccination, recurring positivity testing, business, office, and school capacity limitations/curtailment, and/or social distancing;
- Public fear and hesitancy to return to offices, schools, and public places, disproportionately affecting the most sensitive populations including our seniors and those with underlying medical conditions;
- Inadequate risk assessment tools to quantify actionable indoor infection risk; and,
- Frequently non-existent regulatory authority and risk assessment, communication, and mitigation standards for indoor air – including public health, environmental, and social welfare agencies in all jurisdictions.

In contrast to the health risk-based regulatory framework and protections for environmental exposures (discussed below), there are no established health risk-based indoor air quality (IAQ) regulatory standards for pathogen exposure in non-health care buildings and public spaces. This is in spite of actual deaths due to COVID-19 respiratory infection approaching 3,000 in one million in the United States, 30x the USEPA’s allowable 70-year excess cancer risk for new source air emissions.<sup>10</sup>

Stringent health risk-based standards are enforced by regulatory agencies for most anthropogenic environmental exposures including ambient (outdoor) air quality, drinking water supply, wastewater and stormwater discharges, and waste/hazardous waste management. USEPA and state/local agencies have established human health risk assessment guidance and requirements for air emissions, hazardous waste management and Superfund sites,<sup>11,12</sup> California’s statewide Proposition 65 safe drinking water<sup>13</sup> and AB2588 air toxic hot spots<sup>14</sup> programs, and the South Coast Air Quality Management District (SCAQMD)’s new source review program for toxic air contaminants.<sup>15</sup>

These and many other regulatory agencies and programs tabulate acute and chronic toxicity hazard indices for a wide range of environmental toxins and multipathway endpoints – for example, excess individual cancer risk is evaluated for sources including factories, roads and highways, wastewater discharge, land disposal sites, deposition of airborne contaminants, and consumer products. Construction and other permits are denied if health risks can not be adequately mitigated.

USEPA<sup>16</sup> and other environmental regulators often adopt standards for excess cancer risk limits ranging 1-100 in one million, representing the likelihood for an individual to contract cancer over 70 years due to a consistent, worst-case or reasonable worst-

<sup>10</sup> <https://www.worldometers.info/coronavirus/>

<sup>11</sup> <https://www.epa.gov/risk/human-health-risk-assessment>

<sup>12</sup> <https://nepis.epa.gov/Exe/ZyPDF.cgi/2000NYYU.PDF?Dockey=2000NYYU.PDF>

<sup>13</sup> <https://oehha.ca.gov/proposition-65>

<sup>14</sup> <https://oehha.ca.gov/air/air-toxics-hot-spots>

<sup>15</sup> <http://www.aqmd.gov/docs/default-source/rule-book/reg-xiv/rule-1401.pdf>

<sup>16</sup> For example, USEPA’s final rule for benzene emissions from various industrial sources (54 Fed. Reg. 38039 published September 14, 1989) states, “In protecting public health with an ample margin of safety under section 112 [of the federal Clean Air Act], EPA strives to provide maximum feasible protection against risks to health from hazardous air pollutants by...limiting to no higher than approximately 1 in 10 thousand [100 in-one-million] the estimated risk that a person living near a plant would have if he or she were exposed to the maximum pollutant concentrations for 70 years.” See [https://archives.federalregister.gov/issue\\_slice/1989/9/14/38039-38082.pdf](https://archives.federalregister.gov/issue_slice/1989/9/14/38039-38082.pdf).

case exposure.<sup>17</sup> In the case of ambient air quality, the SCAQMD requires applicants for new air emission sources to implement Best Available Control Technology for Toxics (T-BACT) to reduce maximum individual cancer risk to below 10 in one million. T-BACT is more stringent than BACT, the criteria pollutant analogue, and requires the most stringent emissions limitation or control technique which is achieved in practice or technologically feasible, suggesting no consideration of cost-effectiveness.

For perspective, USEPA reported<sup>18</sup> the highest excess cancer risk from 2002 air pollution data was 1,200-in-one million over a 70-year lifetime/exposure duration. This result was for Cerritos, California (southeast Los Angeles County), at 34 times the national average. For 2012-13 SCAQMD calculated a peak excess cancer risk of 1,050-in-one million over 70 years, around the ports of Los Angeles and Long Beach.<sup>19</sup> Due to substantive emission control regulations for mobile and stationary sources implemented over the years, this peak 70-year calculated risk had dropped to 842-in-one million by 2018-19, as published in SCAQMD's 2021 Multiple Air Toxics Exposure Study V final report.<sup>20</sup>

Existing USEPA and building code indoor air standards are primarily focused on comfort and energy considerations including fresh air, pollutant and odor removal, temperature, humidity, and energy efficiency.<sup>21</sup> ASHRAE's *Ventilation for Acceptable Indoor Air Quality* standard is "intended to provide IAQ that is acceptable to human occupants and that minimizes adverse health effects,"<sup>22</sup> while the requirements of Table 6-1 (Minimum Ventilation Rates in Breathing Zone) "do not address the airborne transmission of airborne viruses, bacteria, and other infectious contagions."<sup>23</sup>

To address these multiple systemic deficiencies and offer an approach to guide public policy for indoor air respiratory infection health risk, an infectious dose model was developed as presented herein, to characterize respiratory transmission sub-processes and assess the comparative efficacy of a broad range of mitigation alternatives. The model follows a traditional mass balance applied to viable airborne pathogens, coupled with respiratory, transport, and infection dynamics of transmission. The "closed" system is defined as a single occupied room with a continuous pathogen source (infected individual), with inputs and outputs for ventilation and HVAC systems. Well-mixed and localized pathogen concentrations are evaluated, with particular attention to respiratory jet dynamics for proximate and downwind receptors. As discussed below, localized concentrations have not been adequately characterized in the published risk/exposure models reviewed.

## 2.2 Literature Review [\[back to TOC\]](#)

A broad review of recent and pertinent literature revealed no published infectious dose model with rigorous and comprehensive characterization of respiratory infection risk with spatially-variable pathogen exposure; respiratory jet dynamics for proximal and downwind receptors; multifaceted comparative depiction of common mitigation measures including face coverings, social distancing, transparent partitions/windows, natural draft openings (NDOs); bulk air currents in the room; breathing zone pathogen variability; and, treatment, filtration, and/or ventilation with non-equilibrium intake pathogen loadings. A few representative studies, with examples of how they might overestimate or underestimate the risk:

- Peng (2022)<sup>24</sup> provides a mathematical Wells-Riley "box model of infection" for airborne transmission and suggests a risk parameter to characterize the risk of cross-infection. Model results are compared with known outbreak events for COVID-19 and other respiratory pathogens. This model assumes a well-mixed space and acknowledges that it does not apply to (1) rooms with clear directional airflow, and (2) receptors within 2 m proximity, with overlapping breathing zones. (See Section 3.8 and Table 6 for a side-by-side comparison of the Peng risk parameter to the APMI metric proposed herein.)
- Bazant (2021-1)<sup>25</sup> and Bazant (2021-2)<sup>26</sup> discuss deviations from the well-mixed assumption (all the air is instantaneously the same), yet the risk calculation equations and model do not incorporate such deviations. The findings are consistent with the current study in that face masks were found to dramatically reduce short-term transmission risk. For COVID-19,

<sup>17</sup> <http://www.aqmd.gov/docs/default-source/planning/risk-assessment/risk-assessment-procedures-v-7.pdf>

<sup>18</sup> <https://www.dailynews.com/2009/06/24/smog-causes-increased-cancer-risk-in-la-county/>

<sup>19</sup> <https://www.latimes.com/local/la-me-cancer-risk-20141003-story.html>

<sup>20</sup> <https://www.aqmd.gov/docs/default-source/planning/mates-v/mates-v-final-report-9-24-21.pdf?sfvrsn=6>

<sup>21</sup> <https://inspectapedia.com/ventilation/Mechanical-Ventilation-EPA.pdf>

<sup>22</sup> <https://www.ashrae.org/technical-resources/bookstore/standards-62-1-62-2>

<sup>23</sup> ASHRAE Standard 62.1-2019, accessed from <https://www.ashrae.org/technical-resources/standards-and-guidelines/read-only-versions-of-ashrae-standards>

<sup>24</sup> <https://pubs.acs.org/doi/10.1021/acs.est.1c06531?ref=pdf>

<sup>25</sup> <https://www.pnas.org/content/118/17/e2018995118>

<sup>26</sup> <https://ocw.mit.edu/resources/res-10-s95-physics-of-covid-19-transmission-fall-2020/lecture-videos/video-6-0-course-conclusion>

Bazant (2021-1) proposes an indoor safety guideline suggesting that “school transmission would be rare” over 80 hours with masked students and adequate ventilation, suggesting that inhaled SARS-CoV-2 virions remain active for up to 80 hours. (Neither Bazant reference provides evidence that inhaled COVID-19 virions can continue to be infective in the human body for over 10 days of continuing exposure – for comparison, CDC (2021) provides 15-minute exposure guidance based on an incubation period at 24 hours,<sup>27</sup> while Johns Hopkins (2021) suggests 4-6 days.<sup>28</sup>)

- Jimenez (2021)<sup>29</sup> offers an on-line calculator and Monte-Carlo simulation model that considers masks and receptor density, exposure duration, shedding rate, and population data. However, a quantitative infectious dose is not described or presented as adjustable, and downwind considerations are not included.
- Mittal (2020)<sup>30</sup> discusses “the flow physics of COVID-19” and discusses reduced respiratory jet velocity from masks to be a benefit. Mittal does not recognize, as discussed below, that reduced exhale velocity adversely impacts dilution of exhaled pathogens. In addition, this report only casually references filtration and air treatment, social distancing, and atmospheric ventilation/air exchanges.
- Buonanno (2020)<sup>31</sup> suggests a COVID-19 emission and infection risk assessment model, although spatial pathogen loading is not specified and a well-mixed assumption reflects the Wells-Riley equation (Riley 1978)<sup>32</sup> with aerosol droplets “instantaneously and evenly distributed in the room,” and “the geometries, the ventilation, and the locations of the infectious sources” are not considered.
- Jones (2020)<sup>33</sup> provides a qualitative model that addresses social distancing, masks, physical activities, ventilation, and exposure duration. However, it does not account for treatment or filtration, or spatial variations in pathogen loading and does not offer quantitative results.
- Halloran (2012)<sup>34</sup> describes a comprehensive breath plume model that incorporates source and aerosol dynamics including respiratory jet parameters; however, the research was focused on animal exposures, and there is no consideration of mitigation measures.

Clearly there is a need for a unified, comprehensive infectious dose model including all relevant source, transport, fate, and infection-related phenomenon. Henceforth, the following attempts to quantify these factors with a simple-to-use parametric framework. Assumptions for individual terms are presented as examples and may be updated as better information is available – there is recognized uncertainty for significant terms, such as the pathogen shedding rate for an infected individual, quantity of pathogen required to establish an infection, and duration over which pathogen uptake is cumulative towards an infection.

### 2.3 The Fundamental Pathogen Material Balance [\[back to TOC\]](#)

The process of respiratory transmission includes three transient elements – (1) **generation** of respiratory viral particles by an infected, shedding individual (source); (2) **transport** of respiratory viral particles from the source into the common ambient environment; and, (3) **fate** – inhalation uptake of respiratory viral particles by uninfected persons (receptor) leading to infections.

From pathogen generation to transport and fate through ultimate infection in a room with airspace volume  $V$ , the following unified indoor air infectious dose model incorporates mitigation measures such as masks, social distancing, transparent partitions/windows, ventilation including NDOs such as windows and doors, and air treatment/filtration.<sup>35</sup> The model provides a quantitative material balance for pathogenic particle quanta (PPQ)<sup>36</sup> such as influenza or COVID-19 virions, to answer, “How safe is your air?”:

<sup>27</sup> <https://www.cdc.gov/coronavirus/2019-ncov/php/contact-tracing/contact-tracing-plan/appendix.html#contact>

<sup>28</sup> <https://www.acpjournals.org/doi/10.7326/m20-0504>

<sup>29</sup> <http://covid-exposure-modeler-data-devils.cloud.duke.edu/>

<sup>30</sup> <https://www.cambridge.org/core/journals/journal-of-fluid-mechanics/article/flow-physics-of-covid19/476E32549012B3620D2452F30F2567F1>

<sup>31</sup> <https://www.sciencedirect.com/science/article/pii/S0160412020312800?via%3Dihub>

<sup>32</sup> <https://academic.oup.com/aje/article-abstract/107/5/421/58522?redirectedFrom=fulltext>

<sup>33</sup> <https://www.bmj.com/content/370/bmj.m3223>

<sup>34</sup> <https://www.ncbi.nlm.nih.gov/pmc/articles/PMC3352828/>

<sup>35</sup> By incorporating the appropriate shedding rates and other exhalation/inhalation parameters, the source and receptors can be modeled for any combination of activities – breathing, talking, coughing, sneezing, singing, etc. Such activity-specific values should be proportioned for temporal frequency.

<sup>36</sup> Alternatively, the ambient viral load, plaque-forming units (PFUs, e.g., infectious virion particles) or active RNA copies in the case of ssRNA virions such as COVID-19. Experimental quantification methods should rely on analyses that quantify the virulent viral population and not total genetic material unless the particle-to-PFU ratio is known.

$$\begin{aligned}
N(t) &= V \bullet \bar{C}_{PPQ} \\
&= N_{\text{initial}} + N_{\text{generate}} - N_{\text{settle}} + N_{\text{reentrain}} - N_{\text{exhaust}} - N_{\text{treat}} - N_{\text{filter}} - N_{\text{decay}} - N_{\text{inhale}} \\
N(t) &= N_0 + N_G - N_S + N_R - N_E - N_T - N_F - N_D - N_I
\end{aligned}
\tag{Eq. 1}<sup>37</sup>$$

where

$N(t)$	=	airborne PPQ in the room at time $t$ .
$\bar{C}_{PPQ}$	=	average concentration of airborne PPQ in the room (PPQ/volume). Represents well-mixed/stirred-tank conditions.
$N_0$	=	initial airborne PPQ, time $t = 0$ .
$N_G$	=	cumulative airborne PPQ generated (exhaled) by $q_{INF}$ sources. Depends on the nature of infection and pathogen shedding rate, and specific activities (such as breathing, talking, coughing, sneezing, singing).
$N_S$	=	cumulative airborne PPQ settling or deposition on surfaces and fomites. Depends on the total area of surfaces and fomites subject to gravitational settling of PPQ-containing droplets.
$N_R$	=	cumulative deposited PPQ that are reentrained in the air due to surface/fomite agitation, air currents, foot traffic, etc.
$N_E$	=	cumulative PPQ that are permanently exhausted, ventilated, or otherwise discharged from the room, via active or passive air-exchanges including recognized NDOs and the departure from $\bar{C}_{PPQ}$ at exhaust intakes.
$N_T$	=	cumulative airborne PPQ that are actively treated or otherwise rendered inactive. Depends on volumetric air treatment rate and pathogen-specific treatment efficiency and incorporates the departure from $\bar{C}_{PPQ}$ at treatment system air intakes.
$N_F$	=	cumulative airborne PPQ that are permanently filtered out of the room air. Depends on volumetric air filtration rate and pathogen-specific filtration efficiency and incorporates the departure from $\bar{C}_{PPQ}$ at filtration system air intakes.
$N_D$	=	cumulative airborne PPQ that naturally/statistically attenuate by dying or otherwise inactivating (half-life).
$N_I$	=	cumulative airborne PPQ that are inhaled and permanently removed from room air. Depends on the number of receptors breathing in the room, and ultimately guides the infectivity analysis, and incorporates the departure from $\bar{C}_{PPQ}$ at receptor breathing zone location(s) of interest.

## 2.4 Pathogen Generation ( $N_G$ ) [\[back to TOC\]](#)

Respiratory pathogens such as COVID-19 are shed from  $q_{INF}$  infected sources' mouth and nose with shedding rate per breath  $g$ , source breathing rate  $n_B$  (breaths/time/person), and time  $t$ :<sup>38</sup>

$$N_G = g \bullet n_B \bullet q_{INF} \bullet (1 - f_{M-E}) \bullet t \tag{Eq. 2}$$

where  $f_{M-E}$  is the mask exhalation factor (fraction of exhaled PPQ that are prevented from entering the ambient air due to a mask).<sup>39</sup>

Shedding rates vary greatly based on the specific pathogen of interest and source's infection level, activities (relaxed breathing, speaking, meowing, coughing, sneezing, singing, etc.), and type of mask. If  $q_{INF} = 0$ ,  $g$  is necessarily zero as well.

## 2.5 Pathogen Transport ( $N_S$ , $N_R$ ) [\[back to TOC\]](#)

Common observation and knowledge dictates that, once infectious respiratory liquid droplets are exhaled, they may either be (1) exhaled at the natural breath velocity associated with a particular activity into the ambient air, or (2) slowed down/filtered prior to ambient discharge by a mask or other obstruction. In either scenario, the exhaled breath is slightly warmer than typical indoor ambient air, and has a natural loft and dispersive tendency, henceforth creating an expanding and billowing dispersion "cloud" around the exhale point (masks) or from the exhale point (unrestricted respiratory jets, ambient breeze).

<sup>37</sup> As mentioned, critical parameters may be discrete values such as percentiles (median, upper or lower quartile), or probability distributions. For the base case and subsequent comparisons, the present study assesses median value inputs.

<sup>38</sup> The terms "breath" and "breathing" are hereafter used broadly to represent the act of respiration, inclusive of all activities which involve exhalation and inhalation of ambient air.

<sup>39</sup> In theory,  $f_{M-E}$  could be negative over small time scales, as droplets lodged in a mask evaporate and release contained pathogens and aerosols to the ambient air - however, this analysis assumes time-averaged mask performance with  $0 < f_{M-E} < 1.0$ .



Various studies have identified substantial levels of viral RNA and respiratory pathogen particles in exhaled droplets, including aerosols ( $< \sim 5 \mu\text{m}$ )<sup>40</sup> generated during tidal breathing via exhaled breath condensate analysis.<sup>41, 42, 43, 44</sup> The transient cloud from exhalation includes droplets  $> 5 \mu\text{m}$  and aerosols of various diameters, primarily composed of saliva and mucus containing water, electrolytes, lipids, proteins and enzymes, viral species, and cells including pathogens in an aqueous sol-gel phase.<sup>45, 46</sup> Depending on particle size and ambient conditions, these may settle to the ground or onto surfaces, disperse with air currents or diffuse due to spatial concentration differences, and remain suspended in the air for hours. Lingering droplets and aerosols release their moisture through evaporation, thereby becoming smaller and more buoyant, dispersive, and diffusive.

Dispersed airborne PPQ – contained in shrinking droplets – continue to circulate with room currents. Without an active mechanism to remove or inactivate airborne pathogens, contained PPQ remain infectious and accumulate in the air, in approximate proportion to the net PPQ generation rate less the pathogen-specific natural activity decay rate.

The model parameters that characterize transport include settling/deposition and reentrainment -  $N_S$  and  $N_R$ , respectively. Settling is represented as a fraction  $s$  of emitted PPQ (generated and released, excluding any PPQ retained by a face covering):

$$N_S = s \bullet N_G \quad [\text{Eq. 3}]$$

Settling rate is a function of droplet size and settling velocity, which depend on the water evaporation rate (and hence humidity and temperature), convective air currents, and droplet agglomeration or fragmentation. Liquid-phase concentrations of PPQ and other solutes in droplets increase as evaporation progresses, and droplets may desiccate based on humidity and temperature conditions in occupied spaces. Desiccation inherently alters the salt balance in respiratory droplets, and this could contribute to PPQ inactivation.

With respect to agglomeration/coagulation due to interdroplet attractions<sup>47</sup> or fragmentation due to collisions between aerosol droplets, these factors are estimated as not significant as exhaled breath droplets in the air are small and quickly diluted in air. The mean free path between aerosol droplets collisions  $\lambda_{\text{MFP}}$  is defined by the collision cross-section  $\sigma$  ( $= 2\pi r_D^2$  with  $r_D$  = maximum droplet radius) and number density of aerosol droplets in a respiratory jet  $\rho_D = g/\dot{V}_i$ , where  $\dot{V}_i$  represents the tidal volume per breath (assumed equal for inhalation and exhalation), the mean free path  $\lambda_{\text{MFP}}$  between droplet collisions is given by:

$$\begin{aligned} \lambda_{\text{MFP}} &> 1/(\sigma \bullet \rho_D) \\ \lambda_{\text{MFP}} &> 1/(2\pi r_D^2 g/\dot{V}_i) \end{aligned} \quad [\text{Eq. 4}]$$

With  $r_D = 2.5 \mu\text{m}$  and  $\dot{V}_i = 500 \text{ ml}$

$$\lambda_{\text{MFP}} > (1.3 \times 10^7/g) \text{ meters}$$

For  $\lambda_{\text{MFP}}$  to be on the order of 1 m (beyond which exhaled breath substantially dissipates, and the probability of collisions or interdroplet attractions diminishes rapidly), droplet agglomeration and fragmentation would not be a significant unless the number of exhaled droplets  $< 5 \mu\text{m}$  approached 13 million droplets per breath.

Reentrainment of settled particles, which may result from people walking, room airflow, and other physical movement of people or objects that agitates depositional surfaces, is expressed as a fraction  $r$  of PPQ settled:

$$N_R = r \bullet sN_G \quad [\text{Eq. 5}]$$

If desired,  $r$  may be characterized as a function of the number of people and type of activity in the room.

<sup>40</sup> Aerosols are a subset of particulate matter (PM), a common but not necessarily equivalent parameter. PM is used in air pollution science and engineering – for example, regulatory ambient (atmospheric) air quality standards for  $\text{PM}_{10}$  and  $\text{PM}_{2.5}$ , where the subscript represents maximum particle diameter in microns. The term “fine PM” means  $\text{PM}_{2.5}$ . Aerosols with diameter  $< 5 \mu\text{m}$  are a component of  $\text{PM}_{5.0}$  and may be predominant for indoor controlled environments.

<sup>41</sup> <https://journals.plos.org/plosone/article?id=10.1371/journal.pone.0002691>

<sup>42</sup> <https://pubmed.ncbi.nlm.nih.gov/19626609/>

<sup>43</sup> <https://www.nature.com/articles/s41591-020-0843-2>

<sup>44</sup> <https://www.ncbi.nlm.nih.gov/pmc/articles/PMC5798362/>

<sup>45</sup> <https://www.ncbi.nlm.nih.gov/pmc/articles/PMC7094568/>

<sup>46</sup> <https://www.ncbi.nlm.nih.gov/pmc/articles/PMC1455483/>

<sup>47</sup> Various cohesive phenomena may be relevant for respiratory droplets, such as dipole moments, hydrogen bonding, static charges, and ionic crystalline shell due to evaporation. Alternatively, evaporation could result in colloidal film skins for aerosols, in which case cohesive attraction may be minimized. No evidence was found to suggest that evaporation has any irreversible impact on PPQ activity or infectivity.

## 2.6 Pathogen Fate ( $N_E$ , $N_T$ , $N_F$ , $N_D$ , $N_i$ ) [\[back to TOC\]](#)

Active pathogen particles that persist in the room air distribute in the entire room volume via diffusion, air currents, and natural convection. Without continuous removal or inactivation of pathogens at a rate faster than the net generation rate  $\dot{N}(t)$ , pathogen levels will continue to persist and/or accumulate in the room air over time, adjusted for the natural decay rate. This is the basis for exposure duration-based guidance, such as the CDC's 15-min published exposure threshold for potential cross-infection from sources.<sup>48</sup>

$\bar{C}_{PPQ}$  represents the average concentration of airborne PPQ in the room per the well-mixed assumption, and spatial variation in pathogen loading is separately addressed with zone factors,  $f_{Z-j}$ . These factors are defined as the ratio of PPQ concentration  $\hat{C}_{PPQ-j}$  at location  $j$ , such as a ventilation intake, treatment/filtration system inlet, or receptor-specific localized breathing zone, to  $\bar{C}_{PPQ}$ :

$$f_{Z-j} = \hat{C}_{PPQ-j} / \bar{C}_{PPQ} \quad [\text{Eq. 6}]$$

$f_{Z-j}$  may be a function of spatial position, time, treatment/filtration system capture efficiency for generated airborne PPQ, and the location of people relative to the source (in the case of  $N_i$ , to address proximal or downwind exposure).

With respect to pathogen fate, five pathways may result in removal of the pathogen particle from the room – exhausted to the atmosphere, treatment, filtration, natural decay, and inhalation –  $N_T$ ,  $N_F$ ,  $N_D$ , and  $N_i$ , respectively.

### 2.6.1 Atmospheric Ventilation

The PPQ permanently exhausted out of the room is determined from the volumetric exhaust ventilation rate  $\dot{V}_E$ , and PPQ concentration  $\hat{C}_{PPQ-E}$ , or alternatively the exhaust-specific zone factor  $f_{Z-E}$  and average bulk concentration  $\bar{C}_{PPQ}$ :

$$\begin{aligned} N_E &= \int \dot{V}_E \cdot \hat{C}_{PPQ-E} dt \\ &= \int \dot{V}_E \cdot f_{Z-E} \cdot \bar{C}_{PPQ} dt \end{aligned} \quad [\text{Eq. 7}]$$

In addition to forced ventilation,  $\dot{V}_E$  may incorporate NDOs including quantifiable air flowrates through windows, doors, and other air gaps. Because NDOs inherently create localized air currents and variance from well-mixed conditions,  $f_{Z-E}$  should incorporate the NDO contribution to departures from  $\bar{C}_{PPQ}$  at all exhaust point locations.

### 2.6.2 Treatment, Filtration

The impact of treatment or filtration is determined from the volumetric airflow through the treatment/filtration system(s),  $\dot{V}_T$  or  $\dot{V}_F$ , treatment/filtration-specific zone factor  $f_{Z-T}$  or  $f_{Z-F}$ , and pathogen control efficiency of the system (removal from the air stream or inactivation), expressed as fractions  $e_T$  and  $e_F$ .<sup>49</sup>  $f_{Z-T}$  and  $f_{Z-F}$  characterize airborne PPQ capture efficiency of the treatment/filtration system. Assuming the airflows and control efficiencies are independent of PPQ concentration, the quantities of airborne PPQ treated or filtered are:

$$N_T = \int e_T \cdot \dot{V}_T \cdot f_{Z-T} \cdot \bar{C}_{PPQ} dt \quad [\text{Eq. 8}]$$

$$N_F = \int e_F \cdot \dot{V}_F \cdot f_{Z-F} \cdot \bar{C}_{PPQ} dt \quad [\text{Eq. 9}]$$

### 2.6.3 Natural Decay

The decay rate of airborne biological PPQ,  $\dot{N}_D$ , occurs at a rate proportional to its current value, hence it follows an exponential profile with PPQ gross<sup>50</sup> decay constant  $\lambda_D$  and half-life,  $t_{1/2}$  – there is no zone factor applicable to this statistical decay process.  $\lambda_D$  is

<sup>48</sup> <https://www.cdc.gov/coronavirus/2019-ncov/php/contact-tracing/contact-tracing-plan/appendix.html#contact>

<sup>49</sup> ACH traditionally represents exhaust ventilation rate for a given indoor space:  $ACH = 60 \cdot \dot{V}_E f_{Z-E} / V$ . While this parameter is useful for characterization of bulk constituent refresh rates in the air, such as for  $H_2O$ ,  $CO_2$ ,  $O_2$ , allergens, indoor/outdoor air pollutants, aerosols, and pathogens, it does not account for mitigation measures specific to airborne pathogens, such as treatment or filtration. A unified, or equivalent ACH is considered ( $ACH_e$ ) to represent active depletion pathways specifically for pathogens (excluding natural decay):  $ACH_e = 60 \cdot (\dot{V}_E f_{Z-E} + e_T \dot{V}_T f_{Z-T} + e_F \dot{V}_F f_{Z-F} + p \dot{V}_i f_{Z-i}) / V$ . See [Section 3.7](#) for a comparative review of this model/ $ACH_e$  with CADR/ACH.

<sup>50</sup> Incorporating all natural statistical decay processes for pathogen inactivation, such as exposure to ionizing, oxidizing, or chemical elements in the air, desiccation/salt balance, and thermal degradation.

representative of a specific pathogen under specific conditions, and may vary based on evaporation dynamics and factors such as air currents, temperature, and humidity:<sup>51</sup>

$$\lambda_D = -[\ln(1/2)]/t_{1/2} \quad [\text{Eq. 10}]$$

$$\dot{N}_D = \lambda_D N(t)$$

$$N_D = (V/t_{1/2})(\ln 2) \int \hat{C}_{PPQ} dt \quad [\text{Eq. 11}]$$

#### 2.6.4 Inhalation and the Respiratory Jet

The final depletion term for pathogen fate,  $N_i$ , represents PPQ that are inhaled by room occupants – a critical parameter that establishes the infectivity of room air relative to the pathogen-specific infectious respiratory dose,  $U_{PPQ}$  (discussed in the following section). Bahl<sup>52</sup> documents COVID-19 airborne PPQ-laden droplets up to 26 ft from a source, hence proximity and downwind considerations are important and potentially significant for respiratory transmission.

For  $p > 1$  people in the room inhaling at an average volumetric rate  $\dot{V}_i \bullet n_B$ , with mask inhalation factor  $f_{M-I}$  (fraction of proximal PPQ not inhaled due to a mask), inhalation-specific breathing zone factor  $f_{Z-I}$  (representing departure from average airborne concentration in the breathing zone), and proximity and downwind source terms for elevated local PPQ concentrations at distance  $x$  from the source,<sup>53</sup> and  $\hat{C}_x$  for  $q_R < p$  proximal or downwind<sup>54</sup> receptors:

$$N_i = [p(1 - f_{M-I})\dot{V}_i n_B \bullet \int f_{Z-I} \hat{C}_{PPQ} dt] + [q_R(1 - f_{M-I})\dot{V}_i n_B \bullet \int (\hat{C}_x - f_{Z-I} \hat{C}_{PPQ}) dt] \quad [\text{Eq. 12}]$$

$\hat{C}_x$  varies with  $x$  as the respiratory cone volume spatially equilibrates to  $\hat{C}_{PPQ}$  – importantly, with no localized accumulation – and respiratory jets are exhaled as regular pulses that can be represented here as steady-state, standing PPQ concentration wavefronts.<sup>55</sup> Respiratory jets, also described as “invisible air bridges,”<sup>56</sup> are modeled with an infectious person at a fixed position in the room, as a horizontal cone centered at mouth/nose height, and with varying proximal/downwind concentrations that are fixed in time while the source is present:

$$N_i = (1 - f_{M-I})\dot{V}_i n_B \bullet [(p - q_R) \int f_{Z-I} \hat{C}_{PPQ} dt + q_R \hat{C}_x t] \quad [\text{Eq. 13}]$$

The exhaled volumes and PPQ concentrations are characterized per dispersion dynamics of a respiratory jet over horizontal distance  $x$ , as the ratio of exhaled single-breath PPQ that remains airborne whilst the respiratory jet disperses away from a single source ( $q_{INF} = 1$ ), to the distributed/expanded volume  $V_x$  of the single breath respiratory jet at  $x$ .<sup>57</sup> Proximal and downwind concentrations are then determined from parametric representation of  $V_x$ :

$$\hat{C}_x = g(1 - s)(1 - f_{M-E})/V_x \quad [\text{Eq. 14}]$$

Exhaled respiratory jets have higher moisture content, temperatures, velocities, and PPQ concentrations than the ambient indoor air. Hence  $V_x$  is affected by the transfer dynamics of excess moisture (evaporation), heat (dissipation), mass (diffusion), and momentum (resistance) of exhaled breath and airborne PPQ-containing droplets, as the respiratory jet equilibrates with ambient room air.

#### 2.6.5 Evaporation of Moisture

The settling fraction  $s$  accounts for settling of PPQ contained in droplets larger than  $5 \mu\text{m}$ . The size cutoff incorporates all droplets that (1) are exhaled as  $< 5 \mu\text{m}$  aerosols, and (2) all larger exhaled droplets that evaporate to  $5 \mu\text{m}$  or less before settling out of the air. Chaudhury<sup>58</sup> suggests 30-50  $\mu\text{m}$  is the transition from evaporation- to deposition-dominated droplet fate. Evaporation, which

<sup>51</sup> For the influence of humidity and temperature effects upon SARS-CoV-2 aerosols, see equations 1/2 in Dabisch 2020:

<https://www.tandfonline.com/doi/full/10.1080/02786826.2020.1829536>.

<sup>52</sup> <https://www.ncbi.nlm.nih.gov/pmc/articles/PMC7184471/>

<sup>53</sup> For distancing below 4.5 ft, this represents minimum sustained face-to-face distance between a shedding individual and a receptor. Sustained is defined as cumulative daily exposure over 15 minutes, with any continuous exposure exceeding 1 minute.

<sup>54</sup> For example, if receptors are between the source and an HVAC return air grille in or near the breathing zone, or an NDO with outward air flow.

<sup>55</sup> The time scales of respiratory pulses and relevant dispersive mechanisms are all on the order of a few seconds – including settling, evaporation, and heat/mass/momentum transfer to the ambient air. No localized accumulation and steady-state assumptions are supported by the consistent time scales.

<sup>56</sup> <https://www.washingtonpost.com/opinions/2021/12/17/stop-pandemic-remove-invisible-air-bridge/>

<sup>57</sup>  $q_v t$  is the inhaled volume of air by  $q$  receptors that are proximal or downwind of the source over  $t$  (neglecting the volume of PPQ and other airborne droplets/particles that may adhere to the outside of masks during inhalation).

<sup>58</sup> <https://www.ncbi.nlm.nih.gov/pmc/articles/PMC7327718/>

depends on air currents, temperature, and humidity in the room air, may alter the survivability and half-life decay of airborne pathogens. Such decay effects are discussed with  $\lambda_D$  above.

## 2.6.6 Heat Dissipation and Thermal Buoyancy

Heat dissipation due to the temperature difference between exhaled breath and room air affects the dispersion of exhaled breath, including both latent heat (evaporation) and sensible heat transfer (contraction). As warm breath cools, assumptions include ideal gas behavior with isobaric conditions, only convective heat transfer, negligible latent heat of a small volume of evaporated moisture, exhaled air at 94°F and ambient at 68°F, for an initial temperature difference  $\Delta T = T_E - T_\infty = 94^\circ\text{F} - 68^\circ\text{F} = 26^\circ\text{F}$ . The breath cloud density  $\rho$  contracts by approximately 5% due to cooling, at a rate proportional to  $\Delta T$ :

$$\begin{aligned}\Delta\rho &\propto \Delta T = (T_E - T_\infty)/T_\infty \\ &= (554^\circ\text{R} - 528^\circ\text{R})/528^\circ\text{R} \\ &= 0.049\end{aligned}\quad [\text{Eq. 15}]$$

This model assumes a homogeneous respiratory jet cone, as well as incompressible gases. Because the cone volume is derived from observational measurements, it reasons the density reduction effect is built into the parametric volume calculation.

The elevated temperature of exhaled breath results in a buoyant force and loft that causes the respiratory cone to rise as it cools, with an initial horizontal release for mouth breathing and slightly below horizontal for nasal breathing.

As discussed below, the model characterizes the respiratory cone in the breathing zone with an approximate horizontal orientation. Because the cone is assumed homogeneous in time but varying spatially as it expands, the pitch is not so critical – the cone encompasses the breathing zone for receptors that are over 3 ft away, even if there is a slight upward or downward pitch.

## 2.6.7 Mass Diffusion

Fickian diffusion of PPQ-containing exhaled breath aerosols into ambient room air is driven by the aerosol fugacity  $f_{A,j}$  difference. Assuming the aerosols (and PPQ) remain uniformly distributed in exhaled breath as it disperses, the initial aerosol fugacity difference is proportional to the concentration gradient:

$$\Delta f_{A,j} \propto \hat{C}_{j,x} - f_{Z,i}\hat{C}_{PPQ} \quad [\text{Eq. 16}]$$

Tsuda<sup>59</sup> calculates Einstein-Stokes diffusion coefficients for spheres  $> 0.05 \mu\text{m}$  (50 nm) to be under  $2.3 \times 10^{-5} \text{ cm}^2/\text{sec}$ , with one-second diffusion distances  $< 50 \mu\text{m}$ . Hence, on the time scale between respiratory jet pulses of seconds, and the associated bulk momentum, mass diffusion is not a significant contribution to  $V_x$ .

## 2.6.8 Momentum Transfer

The outward momentum of respiratory jets is transferred to the surrounding air as exhaled air moves away from the source. Jet momentum diminishes over seconds due to resistance from the surrounding ambient air. Various researchers have analyzed respiratory jet dynamics with unmasked subjects – Tang's shadowgraph Schlieren image technique (Tang 2013)<sup>60</sup> characterizes the horizontal momentum of respiratory jets with spread angles from nasal/mouth breathing at 25-48°, and sneezing or coughing at 76-80°. Gupta<sup>61</sup> measured visible exhale spread angles for cigarette breathing of 21-23° for nasal breathing (2 jets) and 30° for mouth breathing. Kwon<sup>62</sup> found initial exhaled velocity vector angles of 49-78° for speaking and 32-38° for coughing.

**Table 1. Average respiratory jet velocity and propagation distance.** (Tang 2013)

Time sec	Mouth Breathing		Nasal Breathing	
	Distance ft	Velocity ft/min	Distance ft	Velocity ft/min
0.0	0.0	120	0.0	180
0.5	0.95	75	0.95	79
1.0	1.6	49	1.5	39
1.5	1.6	45	1.5	24
2.0	1.6	24	1.7	16

<sup>59</sup> <https://www.ncbi.nlm.nih.gov/pmc/articles/PMC4398662/>

<sup>60</sup> <https://www.ncbi.nlm.nih.gov/pmc/articles/PMC3613375/>

<sup>61</sup> <http://edge.rit.edu/content/P13051/public/Research%20Notes/Characterizing%20Exhaled%20Airflow%20from%20Breathing.pdf>

<sup>62</sup> <https://www.ncbi.nlm.nih.gov/pmc/articles/PMC7112028/>



Mazzino 2021<sup>63</sup> characterizes the respiratory jet evolving into turbulent puffs in seconds, supporting the well-mixed hypothesis for dispersing respiratory air volume. Taking the respiratory jet as an approximately horizontal right cone with apex at the source (assumed 30° for the initial respiratory jet in quiescent conditions, without mitigation) and uniform PPQ concentration as it expands, analogous to Gaussian plume geometry,  $V_x$  is a function of  $x$ , the horizontal velocity-adjusted respiratory jet cone apex angle  $\theta$ , and mask/vertical airflow angle expansion factor  $f_{M-\theta}$ .<sup>64</sup>

$$V_x = f_v \cdot (\pi x^3/3) \cdot \tan^2(f_{M-\theta} \cdot \theta/2)/\text{breath} \quad [\text{Eq. 17}]$$

$f_{M-\theta}$  is a correction for  $\theta$  when the source is wearing a mask, a transparent partition separates the source from receptors, or there is other directed vertical airflow ( $f_{M-\theta} < 180^\circ$ ), and volume correction factor  $f_v$  accounts for limitations of Schlieren imaging. With respect to  $V_x$  and  $\theta$ , the downwind respiratory jet cone will be stretched if there is a prevailing horizontal air velocity or breeze across the source.

Tang measured respiratory jet propagation with quiescent room conditions – Table 1 provides average nasal/mouth breathing respiratory jet velocity and propagation distance (complete vectors, including horizontal and vertical components) estimated from Tang Figures 4A/5A.

Tang, Xu,<sup>65</sup> and others<sup>66</sup> note the Schlieren technique underestimates propagation of exhaled respiratory jets, as it relies on a minimum difference between respiratory jet transient temperature and  $T_\infty$  of at least 15°F. Quoting, “maximum propagation distances can only be observed whilst there remains a temperature difference between the exhaled and ambient laboratory air.” Assuming the quoted propagation values represent remaining exhaled breath at >79°F (with  $T_\infty = 64^\circ\text{F}$ ), any breath cooler than 79°F is not visualized using Schlieren. To account for this, an estimated 50% of exhaled air initially at  $T_E = 94^\circ\text{F}$  has cooled sub-79°F, with resulting volume correction factor  $f_v = 2.0$ .<sup>67</sup>

The total horizontal velocity vector  $v_{H,T}$  equals the ventilation-induced ambient component  $v_{H,A}$  plus the respiratory component  $v_{H,R}$  with mask velocity retardation factor,  $f_{M-v}$ :

$$v_{H,T} = v_{H,A} + (f_{M-v} \cdot v_{H,R}) \quad [\text{Eq. 18}]$$

As depicted in Table 1, respiratory jets from mouth and nasal breathing have similar distance and velocity profiles over time. Assuming these results are reasonable approximations (say, within 5%) of the horizontal velocity component, curve fitting of these results provides a parametric representation of velocity as a function of distance over the first two seconds:<sup>68</sup>

- Mouth breathing - linear curve fit with  $r^2 = 0.93$  yields  $x = 2.4$  ft with average  $v_{H,R} = 61$  ft/min.
- Nasal breathing - quadratic curve fit with  $r^2 = 0.99$  yields  $x = 1.9$  ft with average  $v_{H,R} = 82$  ft/min.

Aswegan<sup>69</sup> suggests that typical thermal comfort design air velocities  $v_{H,A}$  pursuant to ASHRAE<sup>70</sup> should not exceed 30-48 ft/min depending on cooling or heating conditions – this could be higher if a receptor is directly in between the source and an HVAC intake register or an open window/NDO with outward air flow.

The downwind jet cone volume will be stretched horizontally but not vertically, resulting in a narrowing  $\theta$  as breeze velocity is increased. Assuming the cone stretch varies linearly with average horizontal velocity over the first two seconds of a respiratory jet,  $\theta$

<sup>63</sup> <https://journals.aps.org/prl/abstract/10.1103/PhysRevLett.127.094501#fulltext>

<sup>64</sup> The effect of a transparent partition or window is incorporated as expansion of the respiratory jet dispersion angle, up to 180°, depending on placement and size relative to the source-receptor pathway.

<sup>65</sup> <https://www.ncbi.nlm.nih.gov/pmc/articles/PMC7111220/>

<sup>66</sup> <https://journals.plos.org/plosone/article?id=10.1371/journal.pone.0034818>

<sup>67</sup>  $(94^\circ\text{F} - 64^\circ\text{F})/(79^\circ\text{F} - 64^\circ\text{F}) = 2.0$ .

<sup>68</sup> This is not to suggest that the respiratory jet stagnates when the measured velocity curve approaches zero. Continuous jet pulses from subsequent exhalations will continue to push the exhaled air out away from the source, even in the absence of a prevailing breeze or other physical movement in the room. Tang's shadowgraph technique has limitations when the exhaled breath cools to and ambient temperature, and velocities below 10-15 ft/min may not be detectable.

<sup>69</sup> <https://www.constructionspecifier.com/designing-for-comfort-iaq-air-distribution-per-ashrae-55-and-62-1/>

<sup>70</sup> American Society of Heating, Refrigeration, and Air-Conditioning Engineers, 55-2013, Thermal Environmental Conditions for Human Occupancy. See also ASHRAE 62.1-2013, Ventilation for Acceptable Indoor Air Quality Addendum p ([https://www.ashrae.org/file\\_library/technical\\_resources/standards\\_and\\_guidelines/standards\\_addenda/62\\_1\\_2013\\_p\\_20150707.pdf](https://www.ashrae.org/file_library/technical_resources/standards_and_guidelines/standards_addenda/62_1_2013_p_20150707.pdf)).

is characterized based on the ratio of respiratory jet velocity and total velocity, along with the respiratory jet cone angle  $\theta_Q$  for unmasked breathing in quiescent ambient conditions:<sup>71</sup>

$$\theta = 2 \tan^{-1}[(f_{M-V} V_{H,R} / V_{H,T})^{3/2} \tan(\theta_Q/2)] \quad [\text{Eq. 19}]$$

In the ideal case,

$$f_{M-V} = \{[\tan(\theta/2)]/[\tan(f_{M-\theta} \bullet \theta/2)]\}^{3/2}$$

This is not achieved in practice, as it is a theoretical extreme that assumes the volume of respiratory jet cones is not affected by mechanisms that create vertical dispersion, with idealized geometric symmetry. In actuality, the discharge point(s) from a nose, mouth, or mask are not radially uniform so there is no true symmetrical cone. Even with  $f_{M-\theta}$  approaching or potentially exceeding 180°, there will be non-zero forward exhale air velocity from any standard mask including N95 – otherwise there would be an unsatisfactory resistance to breathing.<sup>72</sup> For the purposes of this model, an arbitrary default minimum is set with  $f_{M-V} > 0.10$ .

### 2.6.9 The Inhalation Equation

This analysis characterizes respiratory jet momentum transfer based on published shadowgraph measurements. Evaporation is incorporated in the settling fraction  $s$ , and mass transfer has been shown to be insignificant. Because dimensions of the modeled horizontal respiratory jet cone are derived from visual observations, the contraction due to heat transfer/cooling is also incorporated in the momentum transfer equations presented here.

Combining terms back into Eq. 13:

$$N_I = (1 - f_{M-I}) \dot{V}_{InB} \bullet [(p - q_R) \int f_{Z-I} \bar{C}_{PPQ} dt + (q_R/V_x)(1 - f_{M-E})(1 - s)gt] \quad [\text{Eq. 20}]$$

with  $V_x$  obtained from Eq. 17 (and associated  $\theta$  from Eq. 19). The proximity and downwind contributions are combined, as the respiratory cone establishes a geometric foundation for both proximal and downwind exposure cones within the breathing zone.

### 2.6.10 Face Coverings, Partitions

Three impacts of face coverings include:

- Aerosol/PPQ filtering;
- Increased respiratory cone apex angle; and,
- Reduction of respiratory jet forward momentum.

Aerosol/PPQ filtering upon inhalation can be described by the fitted filtration efficiency (FFE) of a particular face covering. The table provided by Clapp<sup>73</sup> shows the wide range of FFE for similar masks worn differently – overall ranging 26-80% and 98% for N95 respirators and 20-3,000 nm aerosols. For exhalation, Asadi<sup>74</sup> reports 90% for surgical masks and only 74% for N95 respirators with 300-20,000 nm aerosols and droplets.

Momentum reduction increases short-term exposure risk because exhaled aerosols linger in the proximity of the source in a more concentrated volume. Inouye<sup>75</sup> concludes that “even the cheapest paper masks” can reduce exhale velocity by over 90% ( $f_{M-V} < 0.10$ ).<sup>76</sup> Viola<sup>77</sup> concludes a front flow volume reduction of over 63% for various face coverings (excluding respirators), subject to limitations of the Schlieren technique (results may understate the actual reduction). With respect to respiratory cone angles, Viola observes supplemental “leakage flow” jets emanating around the edges of face coverings, so a specific cone angle impact is not specified. Depending on the type of face covering, the predominant release direction may be upward from a source’s brow, downward from the neck area, or even backward.

<sup>71</sup> Assuming  $\theta_Q$  is properly characterized by Schlieren imaging, without the need for a correction as for the respiratory jet cone volume.

<sup>72</sup> In the case of impervious masks with specific vent/filter holes or cartridge filters, characterization of respiratory jets would require special assessment.

<sup>73</sup> <https://jamanetwork.com/journals/jamainternalmedicine/fullarticle/2774266>

<sup>74</sup> <https://www.nature.com/articles/s41598-020-72798-7>

<sup>75</sup> <https://www.niid.go.jp/niid/JJID/59/179.pdf>

<sup>76</sup> This respiratory jet model assumes the jet expansion is conical with spatially homogeneous PPQ concentration. Values of  $f_{M-V}$  below 0.10 are not realistic due to the incompressible gas assumption.

<sup>77</sup> <https://arxiv.org/pdf/2005.10720>

Considering all these discharge directions as well as airflow in the horizontal plane,  $f_{M-\theta}$  may be expected to result in a consolidated respiratory jet release angle  $f_{M-\theta} \bullet \theta$  baseline exceeding  $120^\circ$ , resulting in significant dilution of the proximal or downwind respiratory jet PPQ concentration, which is partly offset by the reduced respiratory jet velocity  $v_{H,R}$ .

An impervious partition structure between source and receptor will spread the respiratory jet cone angle, resulting in substantial dilution enhanced by turbulence as the respiratory jet reflects upon the structure. Openings or cross flow across partition edges can be incorporated with the bulk air velocity  $v_{H,A}$ , at the perpendicular plane edge of the partition.

PPQ that deposit on the outside surface of a mask are not considered to be eliminated from the air. While airborne PPQ may adhere to the mask upon inhalation, the assumption is those PPQ are released back into the air upon exhalation – hence receptors wearing masks results in a nominal increase in  $N(t)$  without masks. The only PPQ excluded from the airborne pathogen load are those captured by a mask from the infected source upon exhalation.

## 2.7 Unified Infectious Dose Model ( $N(t)$ , $\alpha$ , $\beta$ , $U_{PPQ}$ , $U_{INF}$ , $t_{INF}$ ) [\[back to TOC\]](#)

Combining all terms into Eq. 1, and assuming volumetric flowrates of exhaust ventilation, treatment/filtration, and inhalation, as well as zone factors and efficiencies of treatment/filtration are not time-variant:<sup>78</sup>

$$\begin{aligned} N(t) &= N_0 + N_G - N_S + N_R - N_E - N_T - N_F - N_D - N_i \\ &= N_0 + [(1-s) + rs]q_{INF} - (q_R/V_x)(1-s)(1-f_{M-i})\dot{V}_i(1-f_{M-E})n_{Bg} \\ &\quad - (1/V)[\dot{V}_{EFZ-E} + e_T\dot{V}_Tf_{Z-T} + e_F\dot{V}_Ff_{Z-F} + (V/t_{1/2})(\ln 2) + (1-f_{M-i})(p-q_R)\dot{V}_i n_{BfZ-i}] \int N(t)dt \end{aligned}$$

with  $V_x$  and associated  $\theta$  determined from Eqs. 17 and 19, respectively. Setting coefficients:

$$\alpha = \{[(1-s) + rs]q_{INF} - (q_R/V_x)(1-s)(1-f_{M-i})\dot{V}_i(1-f_{M-E})n_{Bg} \quad \text{[Eq. 21]}$$

$$\beta = (1/V)[\dot{V}_{EFZ-E} + e_T\dot{V}_Tf_{Z-T} + e_F\dot{V}_Ff_{Z-F} + (V/t_{1/2})(\ln 2) + (1-f_{M-i})(p-q_R)\dot{V}_i n_{BfZ-i}] \quad \text{[Eq. 22]}$$

and differentiating over time:

$$\begin{aligned} N(t) &= N_0 + \alpha t - \beta \int N(t)dt \\ \dot{N}(t) &= \alpha - \beta N(t) \end{aligned}$$

The solution to this linear, first-order differential equation is obtained using a substitution method, with integration constant  $k$  determined from the initial boundary condition:

$$\begin{aligned} N(t) &= ke^{-\beta t} + (\alpha/\beta) \\ N(t_0) &= N_0 \\ k &= N_0 - (\alpha/\beta) \end{aligned}$$

Thus:

$$N(t) = [N_0 - (\alpha/\beta)]e^{-\beta t} + (\alpha/\beta) = N_0 e^{-\beta t} + (\alpha/\beta)(1 - e^{-\beta t}) \quad \text{[Eq. 23]}$$

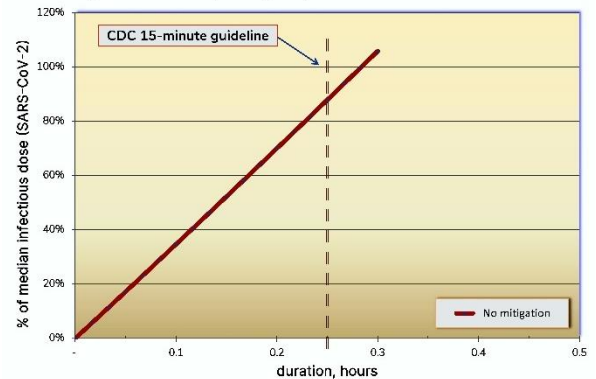
where  $N(t)$  stabilizes and asymptotically tends to  $\alpha/\beta$ , and reaches 90% of the steady-state PPQ loading when  $t \sim 2.3/\beta$  min. Along with known PPQ infectious dose or dose range for a specific pathogen, Eq. 25 below may be solved to determine the maximum exposure time for a typical receptor to avoid infection in a room with particular  $N(t)$  profile and asymptote. Infection risk mitigation strategies may then be compared for effectiveness.

An infection develops when a receptor inhales sufficient, or infectious load, of active pathogen particles. The cumulative uptake of PPQ for all receptors is provided by Equation 20:

$$N_i = (1-f_{M-i})\dot{V}_i n_{B} \bullet [(p-q_R) \int f_{Z-i} \bar{C}_{PPQ} dt + q_R(1-s)(1-f_{M-E})(gt/V_x)]$$

Setting  $p = 2$  and  $q_R = 1$  to reflect one shedding source ( $q_{INF} = 1$ ) and one receptor proximal to or downwind of the source, and assuming  $f_{Z-i}$  is not time-variant, the PPQ uptake by one receptor is  $U_{PPQ}$  (incorporating Eq. 23):

Figure 1. Base case (no mitigation) infectious dose model results.



<sup>78</sup> If any of these parameters vary over time, the model is may be applied incrementally, with end-to-end temporal initial and boundary conditions.

$$\begin{aligned}
 U_{PPQ} &= (1 - f_{M-I})\dot{V}_{inB}[(1/M)f_{Z-I}\int N(t)dt + (1 - s)(1 - f_{M-E})(gt/V_x)] \\
 &= (1 - f_{M-I})\dot{V}_{inB}\{(1/M)(1/\beta)f_{Z-I}[\alpha t + (N_0 - (\alpha/\beta))(1 - e^{-\beta t})] + (1 - s)(1 - f_{M-E})(g/V_x)t\}
 \end{aligned}
 \quad [Eq. 24]$$

Given the inhaled PPQ infectious dose,  $U_{INF}$ , for a particular pathogen,<sup>79</sup> the time to infection  $t_{INF}$  for a given pathogen can be determined implicitly:

$$U_{INF} = (1 - f_{M-I})\dot{V}_{inB}\{(1/M)(1/\beta)f_{Z-I}[\alpha t_{INF} + (N_0 - (\alpha/\beta))(1 - \exp(-\beta t_{INF}))] + (1 - s)(1 - f_{M-E})(g/V_x)t_{INF}\} \quad [Eq. 25]$$

Various indoor air disinfection strategies are discussed in the following section. These are compared for effectiveness using this infectious dose model for a hypothetical classroom and the base case assumptions described below. Input terms and nomenclature for quantitative/numerical determination of  $N(t)$ ,  $U_{PPQ}$ , and  $t_{INF}$  are listed in Table 2; input values, assumptions, and further references are discussed in the following section.

Figure 1 depicts infectious dose results for the base case described below, with no mitigation. 100% of the median infectious dose is inhaled by a receptor at just under 17 min, consistent with CDC's 15-minute close-contact guideline,<sup>80</sup> where close contact is defined as within 6 ft – the base case uses a minimum distance  $x = 4.5$  ft.

At 17 min the source has exhaled around 16,000 net airborne virions that remain infectious (real-time airborne PPQ number), which would represent an uptake of 7 PPQ by a receptor in a well-mixed room under steady state conditions. If the receptor is proximate as in the base case, this model projects an infectious dose uptake of 150 PPQ in 17 minutes – over 95% of the accumulated dose is due to proximity and elevated PPQ concentrations in line of the source's respiratory jet. Without consideration of the spatial variability of PPQ concentration, the pathogen exposure is underestimated > 20x.

## 2.8 Base Case & Assumptions [\[back to TOC\]](#)

### 2.8.1 Model Configuration

Table 2 lists all assumed values for the base case. Because of possibly severe respiratory infections from a given pathogen, the base case assumptions are based on reasonable worst-case assumptions to consider vulnerable receptors such as immunocompromised individuals or those with underlying medical conditions. Where applicable, parameters represent the SARS-CoV-2 nonvariant strain.

The room airspace volume  $V$  is equal to the room volume less volumes occupied by objects or  $q$  occupants. This base case assumes a typical classroom, with floor area  **$A = 1,000 \text{ ft}^2$** , "average" ceiling height  **$H_{avg} = 10 \text{ ft}$** , typical person occupying a volume  **$V_{person} = 2.3 \text{ ft}^3$** ,<sup>81</sup> objects such as desks covering 10% of the floor area ( $a_{objects}$ ) to a height  $H_{objects}$  of 2.5 ft, 30 occupants ( **$p = 30 \text{ persons}$** ):

$$\begin{aligned}
 V &= (A \cdot H_{avg}) - (a_{objects} \cdot A \cdot H_{objects}) - pV_{person} \\
 &= \mathbf{9,700 \text{ ft}^3}
 \end{aligned}$$

The base case assumes a single source entering the room at  $t = 0$  and remaining in the room over the exposure duration, with initial airborne PPQ  **$N_0 = 0$** , infected persons  **$q_{INF} = 1$** , and proximal/downwind receptors  **$q_R = 5$** . An alternate scenario with non-zero  $N_0$  may characterize an uninfected person entering with a pre-existing PPQ airborne concentration or continuing PPQ source in the room. Such cases would consider more steady-state ambient PPQ concentrations, closer to the generation/depletion ratio,  $\alpha/\beta$ .

### 2.8.2 Generation

Respiratory pathogens such as COVID-19 are shed from a source's mouth and nose. Viral and bacterial respiratory shedding rates vary based on the specific pathogen or variant (Reardon 2021),<sup>82</sup> the source's activity and breathing regime, and the extent of symptom presentation. Researchers at Boston University's Medical School estimate that irreversible host lung cell damage occurs within 3-6 hours of initial infection or uptake of COVID-19 virions.<sup>83</sup> The pathology of viral respiratory infections comprises of virus-

<sup>79</sup> The infectious dose  $U_{INF}$  is often represented by  $N_{ID}$  for airborne transmission and infectious diseases or, for median uptake,  $HID_{50}$ , the minimum dose required to initiate infection in 50% of the exposed population.

<sup>80</sup> <https://www.cdc.gov/coronavirus/2019-ncov/php/public-health-recommendations.html>

<sup>81</sup> <https://bionumbers.hms.harvard.edu/bionumber.aspx?s=n&v=3&id=109718>

<sup>82</sup> For example, it is postulated an individual infected with the Delta variant of SARS-CoV-2 may have a viral load > 1,000x higher than that for the original strain (<https://www.nature.com/articles/d41586-021-01986-w>).

<sup>83</sup> <https://www.contagionlive.com/view/coronavirus-damages-lung-cells-in-just-hours>



induced host lung cell lysis, which results in free viral particles that may be exhaled/expelled - hence, an infected source may begin shedding contagious viral particles within a few hours of contracting an infection.

Various researchers have proposed shedding rates for SARS-CoV-2, normal breathing estimates range from a few virions/br to  $> 10^5$  RNA copies/min; see Ma 2020, Alsved 2020, Leung 2020, and Riediker 2020.<sup>84,85,86,87</sup>

This base case assumes one infected, unmasked source breathing normally, with SARS-CoV-2 median and continuous shedding rate  $g = 100 \text{ PPQ/br}$  ( $\sim 1,600 \text{ PPQ/min}$ ),<sup>88</sup> median male/female breathing rate  $n_B = 16 \text{ br/min/pp}$ ,<sup>89</sup> and no mask or face covering for the source ( $f_{M-F} = 0$ ). Considering the orders-of-magnitude variation in the COVID-19 shedding rates from different sources just for normal breathing, and similar range variation with respect to the dose required to establish a COVID-19 infection and unknown breathing characteristics of the source, this infectious dose model is useful for a comparative review of air disinfection strategies.

The shedding rate accommodates any physical activity/breathing type. While it is intuitive that physical activities and labored breathing may generate more virions and aerosols per breath:

- The volume of air per breath is bounded by the maximum pulmonary volume.
- $n_B$  may increase, although more frequent breaths may also be shallower with decreased volume.
- Exhalation momentum encourages air dispersion ( $\theta$  increases with  $v_{H,R}$ ).
- High shedding activities including coughs, sneezes, and labored breathing may create more large droplets that are inclined to settle and would contribute a relatively small number of breaths over extended durations.

### 2.8.3 Depletion, Reentrainment

Researchers have studied the aerosol dynamics of exhaled breath.<sup>90,91</sup> Taiwanese researchers published findings in 2014<sup>92</sup> that exhaled breathing particles (EBPs)<sup>93</sup> from normal breathing of mechanically ventilated patients ranged 0.47-2,600 droplet particles/breath, with all below  $5 \mu\text{m}$  and 80 percent from 0.3-1.0  $\mu\text{m}$ .

2011 Harvard<sup>94</sup> and Queensland<sup>95</sup> studies report comparable results, with respiratory droplets (normal breathing)  $\sim 0.9 \mu\text{m}$ , fairly normal distribution and most particles  $< 4 \mu\text{m}$ . A 2020 Glasgow University survey<sup>96</sup> reports aerosols  $< 3 \mu\text{m}$  are produced in the lower respiratory tract via bronchiolar fluid film bursts and laryngeal region via airflow-induced shear forces over mucosal surfaces, whereas larger droplets to  $500 \mu\text{m}$  are generated in oral/nasal cavities by agitation during coughing, sneezing, or strong vocalizing.

A 2007 Taiwanese study<sup>97</sup> characterizes the size distribution of aerosols from coughing by human subjects, with droplets mostly between 1-10  $\mu\text{m}$ . Scheuch (2020)<sup>98</sup> discusses aerosol settling velocities based on diameter – neglecting ambient or interdroplet charge/electrostatic effects (affinity or repulsive forces), the settling velocity of breathing aerosols  $< 10 \mu\text{m}$  is below 3,000  $\mu\text{m/sec}$ .

Clearly this settling velocity would result in minimal deposition of PPQ aerosols from the breathing zone unless bulk air currents in the room are essentially nonexistent – or in the unlikely case of high impingement velocities upon particularly absorptive surfaces. Aerosol persistence in the air is increased as the droplets shrink due to the evaporation of water. Researchers have characterized the importance of droplet size and evaporation rate on settling, and it is commonly accepted that aerosols below  $5 \mu\text{m}$  tend to stay airborne with a settling half-life exceeding one hour.<sup>99</sup>

<sup>84</sup> <https://www.medrxiv.org/content/10.1101/2020.05.31.20115154v1>

<sup>85</sup> <https://www.tandfonline.com/doi/full/10.1080/02786826.2020.1812502>; see Figure 1, for example.

<sup>86</sup> <https://www.nature.com/articles/s41591-020-0843-2>

<sup>87</sup> <https://jamanetwork.com/journals/jamanetworkopen/fullarticle/2768712>

<sup>88</sup> Any revision to  $g$  should consider a review of  $U_{INF}$ , as both values are highly uncertain but likely correlated.

<sup>89</sup> <https://www.medicalnewstoday.com/articles/324409#adults>

<sup>90</sup> <https://pubs.acs.org/doi/pdf/10.1021/acs.est.1c00235>

<sup>91</sup> <https://www.ncbi.nlm.nih.gov/pmc/articles/PMC3613375/>

<sup>92</sup> <https://www.ncbi.nlm.nih.gov/pmc/articles/PMC3903594/>

<sup>93</sup> Particles in this context mean droplets or aerosols, not individual pathogenic particles.

<sup>94</sup> <https://www.ncbi.nlm.nih.gov/pmc/articles/PMC3123971/>

<sup>95</sup> <https://www.sciencedirect.com/science/article/pii/S0021850211001200#>

<sup>96</sup> <https://www.frontiersin.org/articles/10.3389/fpubh.2020.590041/full>

<sup>97</sup> <https://www.liebertpub.com/doi/10.1089/jam.2007.0610>

<sup>98</sup> <https://www.liebertpub.com/doi/10.1089/jamp.2020.1616>

<sup>99</sup> <https://www.frontiersin.org/articles/10.3389/fpubh.2020.590041/full#B36>

Table 2. List of input terms and nomenclature for the unified infectious dose model.

Symbol	Description	Base Value	Equation	Notes/Reference
<b>Model Configuration</b>				
V	Room air volume	9,700 ft <sup>3</sup>	1	Average ceiling height = 10 ft
T	Elapsed exposure time	(min)	2	Independent variable
N <sub>0</sub>	Initial airborne PPQ at t = 0	0	1	
q <sub>INF</sub>	Number of infected persons (sources)	1 pp	2	q <sub>INF</sub> ≥ 1; if q <sub>INF</sub> = 0, ensure g = 0 below
P	Total number of persons	30 pp	12	p ≥ 2
q <sub>R</sub>	Number of proximal/downwind persons (receptors)	5 pp	12	q <sub>R</sub> < p
<b>Generation</b>				
g	Pathogen shedding rate per breath	100 PPQ/br	2	COVID-19; review in tandem with q <sub>INF</sub> and U <sub>INF</sub>
n <sub>B</sub>	Number of breaths taken by each infected source per unit time	16 br/min/pp	2	Median of 12-20 br/min range
f <sub>M-E</sub>	Exhaled PPQ fraction captured by mask	0.0	2	f <sub>M-E</sub> = 0 if no face covering for source
<b>Depletion, Reentrainment</b>				
s	Fraction of emitted PPQ that settle	0.05	3	0 ≤ s < 1
r	Fraction of settled PPQ that reentrain	0.10	5	0 ≤ r < 1
t <sub>1/2</sub>	PPQ statistical decay half-life	66 min	10	van Doremalen 2020 <sup>100</sup> (nonvariant SARS-CoV-2)
<b>Ventilation, Treatment, Filtration</b>				
Ṡ <sub>E</sub>	Volumetric exhaust ventilation airflow	450 CFM	7	3x CA building energy standard: 0.15 CFM/ft <sup>2</sup>
f <sub>Z-E</sub>	Exhaust-specific zone factor	1.0	7	f <sub>Z-E</sub> = 1.0 if well-mixed
Ṡ <sub>T</sub>	Treatment system volumetric airflow	0 CFM	8	Ṡ <sub>T</sub> = 0 if no treatment
f <sub>Z-T</sub>	Treatment-specific zone factor	1.0	8	f <sub>Z-T</sub> = 1 if well-mixed
e <sub>T</sub>	Treatment system control efficiency	0.999	8	0 ≤ e <sub>T</sub> < 1; typical specification is 0.999
Ṡ <sub>F</sub>	Filtration system volumetric airflow	0 CFM	9	Ṡ <sub>F</sub> = 0 if no filtration
f <sub>Z-F</sub>	Filtration-specific zone factor	1.0	9	f <sub>Z-F</sub> = 1.0 for well-mixed
e <sub>F</sub>	Filtration system control efficiency	0.999	9	0 ≤ e <sub>F</sub> < 1; typical specification is 0.999
ACH <sub>e</sub>	Equivalent ACH (air changes per hour)	(hr <sup>-1</sup> )	31	Calculated
<b>Inhalation</b>				
Ṡ <sub>I</sub> , Ṡ <sub>E</sub>	Tidal volume per breath (inhale/exhale)	0.016 ft <sup>3</sup>	12	Average of 400-500 ml for adults
f <sub>M-I</sub>	Inhalation PPQ fraction captured by mask	0	12	f <sub>M-I</sub> = 0 if no face covering for receptor
f <sub>Z-I</sub>	Inhalation breathing zone factor	1.0	12	f <sub>Z-I</sub> = 1.0 if well-mixed
<b>Proximity &amp; Downwind Considerations</b>				
C <sub>x</sub>	Local PPQ concentration at proximal/downwind receptor	(PPQ/ft <sup>3</sup> )	12	Calculated [Eq. 14]
V <sub>x</sub>	Respiratory jet breath cone volume at receptor distance x	(ft <sup>3</sup> /br)	17	Calculated
f <sub>v</sub>	Volume correction factor	2.0	17	Schlieren observational limitation
x	Minimum distance between source and receptors	4.5 ft	17	3.0 ft < x < 17 ft
f <sub>M-θ</sub>	Mask/partition/vertical airflow angle expansion factor	1	17	f <sub>M-θ</sub> = 1.0 if no source masks, partitions, vertical airflow
f <sub>M-v</sub>	Mask velocity retardation factor	1	18	0.10 < f <sub>M-v</sub> ≤ 1; f <sub>M-v</sub> = 1.0 for no source face covering
V <sub>H,R</sub>	Horizontal respiratory jet velocity, first 2 sec	71 ft/min	18	Average of nasal/mouth breathing (Tang 2013)
V <sub>H,A</sub>	Horizontal bulk air velocity	49 ft/min	18	25-49 ft/min per ASHRAE, default 49 (Section 2.5.8)
V <sub>H,T</sub>	Total horizontal initial velocity of respiratory jet + bulk air	120 ft/min	18	Calculated
θ <sub>Q</sub>	Respiratory jet cone apex angle, no mask, quiescent	30°	19	Tang 2013, etc.
θ	Respiratory jet cone apex angle, no mask, breeze-adjusted	(°)	19	Calculated; ensure f <sub>M-θ</sub> < 180°
<b>Unified PPQ Balance Equation</b>				
α	Generation coefficient, PPQ per unit time	(PPQ/min)	21	Calculated
β	Depletion coefficient, inverse time	(min <sup>-1</sup> )	22	Calculated
<b>Infectious Dose</b>				
U <sub>PPQ</sub>	Cumulative PPQ uptake by a receptor	(PPQ)	24	Calculated
U <sub>INF</sub>	Infectious PPQ dose for a particular pathogen	150 PPQ	25	COVID-19; review in tandem with g
t <sub>INF</sub>	Time for receptor to accumulate infectious dose	(min)	25	Calculated; t <sub>INF</sub> = time to infection
APMI	Airborne Pathogen Mitigation index (APMI; 0-10)	-	33	Calculated from t <sub>INF</sub> for nonvariant SARS-CoV-2

<sup>100</sup> <https://www.nejm.org/doi/10.1056/NEJMc2004973>

Scheuch (2020) further reports the settling distance for aerosols < 5  $\mu\text{m}$  is on the order of 5 cm/min - exhaled particles from relaxed breathing will not experience significant deposition considering room air currents and ongoing evaporation that reduces droplet size. For the base case, a default value is assumed for the settling fraction  **$s = 0.05$** . COVID-19, influenza, and many other common airborne pathogenic quanta < 0.2  $\mu\text{m}$ , so each aerosol droplet down to 0.3  $\mu\text{m}$  has the capacity to contain such virions.

For reentrainment of settled droplets, no quantitative studies were found to adequately characterize reentrainment. Settled particles may land on surfaces or into porous materials such as carpet and other fabrics. These settled particles will continue to desiccate over time and may potentially be disturbed and reentrained in room air as the result of agitation or aerodynamic shear forces. The default reentrainment fraction is assumed at 10 percent of the settled PPQ, or  **$r = 0.10$** .

van Doremalen<sup>101</sup> reports COVID-19 aerosol stability is on the order of hours, with a half-life ranging 1.1-1.2 hours. This base case assumes  **$t_{1/2} = 66 \text{ min}$** . If an estimate is desired based on specific room climate conditions, the US Department of Homeland Security (DHS)<sup>102</sup> offers a SARS-CoV-2 airborne decay tool, which calculates half-life ranging 20-160 min, with maximum persistence with decreasing relative humidity (RH) and temperature, over typical comfort and design guide ranges 30-60%RH and 68-76°F. <sup>103,104</sup>

#### 2.8.4 Ventilation, Treatment, Filtration

For exhausted air from the room, California's 2019 building energy efficiency standard<sup>105</sup> specifies the required fresh air mechanical ventilation rate for general occupancy at 0.15 CFM/ft<sup>2</sup> of conditioned floor area A. Using 3x this minimum standard, the PPQ exhausted quantity  **$\dot{V}_E = 450 \text{ CFM}$** , calculated as follows:

$$\dot{V}_E = 3 \bullet (0.15 \text{ CFM/ft}^2) \bullet A = 450 \text{ CFM}$$

Assuming the exhausted, treated, filtered, and inhaled air have the same PPQ loading as the average PPQ concentration in the room air (well-mixed;  $\bar{C}_{PPQ}$ ), the corresponding zone factors for each airflow are unity:

$$f_{Z-E} = f_{Z-T} = f_{Z-F} = f_{Z-I} = 1.0$$

Volumetric air flowrates and control efficiencies are specific to each treatment or filtration system. A default 99.9% control efficiency is used for each such system ( **$e_T = e_F = 0.999$** ). Treatment and filtration modules are equivalent and can be used interchangeably – for example, if two distinct treatment systems are modeled.

#### 2.8.5 Inhalation

Typical values for male and female adult tidal volume range 400-500 ml/ breath<sup>106</sup> - using the average,  **$\dot{V}_I = \dot{V}_T = 0.016 \text{ CFM/br}$** . The base case assumes no masks ( **$f_{M-I} = 0$** ), and well-mixed zone factors with  **$f_{Z-I} = 1.0$** .

#### 2.8.6 Proximity, Downwind Parameters

For the respiratory jet from the infected source, base case parameters are:

- Horizontal respiratory jet velocity  **$v_{HR} = 71 \text{ ft/min}$**  (average of nasal and mouth breathing as previously discussed)
- Horizontal bulk air velocity  **$v_{HA} = 49 \text{ ft/min}$**  (maximum of ASHRAE recommended range)
- Respiratory jet cone apex angle  **$\theta_Q = 30^\circ$**  (quiescent, no mask)
- Respiratory cone volume correction factor  **$f_v = 2.0$**  (Schlieren adjustment)
- Minimum distance between source and receptors  **$x = 4.5 \text{ ft}$** , as previously noted
- Mask/vertical airflow angle expansion factor  **$f_{M-Q} = 1$**  and mask velocity retardation factor  **$f_{M-V} = 1$**  (no mask)

The range for x is 3-17 ft. This is a limitation of the respiratory cone representation, and realistic for typical exposure scenarios: It is unlikely for receptors to be < 3 ft from a potential infected source for any extended time in public places or offices, and minimum distances > 17 ft are not considered proximate in the context of a 1,000 ft<sup>2</sup> area.

<sup>101</sup> <https://www.nejm.org/doi/10.1056/NEJMc2004973>

<sup>102</sup> <https://www.dhs.gov/science-and-technology/sars-airborne-calculator>

<sup>103</sup> For RH, see [Lennox](#) and [Condair](#). For temperature, see [OSHA](#).

<sup>104</sup> The DHS calculator and curve fitting provide half-life estimates at 30-60%RH for SARS-CoV-2 in air at 59 min for 68°F and 45 min for 72°F.

<sup>105</sup> [https://www.energy.ca.gov/sites/default/files/2021-06/CEC-400-2018-020-CMF\\_0.pdf](https://www.energy.ca.gov/sites/default/files/2021-06/CEC-400-2018-020-CMF_0.pdf)

<sup>106</sup> <https://www.ncbi.nlm.nih.gov/books/NBK482502/>

### 2.8.7 Consolidated Generation/Depletion Coefficients

Generation and depletion coefficients  $\alpha$  and  $\beta$ , respectively, are calculated from the parameters discussed above. Base case values are  $\alpha = 1.485 \text{ PPQ/min}$  and  $\beta = 0.057 \text{ min}^{-1}$ , and the ratio  $\alpha/\beta = 25.924 \text{ PPQ}$  represents the steady-state average PPQ number in the room air achieved once the depletion rate (which is proportional to the ambient PPQ number) equals the generation rate.

### 2.8.8 Infectious Dose Parameters

Cumulative PPQ uptake by an individual receptor  $U_{\text{PPQ}}$  is calculated by the model, and time to the receptor's accumulation of an infectious dose is determined implicitly from the pathogen specific infectious PPQ dose  $U_{\text{INF}}$  and Equation 25. As with the shedding rate  $g$ , there is substantial uncertainty regarding  $U_{\text{INF}}$  for SARS-CoV-2.<sup>107</sup>

Shedding rates and infectious dose values are dependent on pathogen species and variant. While this study is applicable to all airborne respiratory pathogens, the specific model parameters are based on references and citations that attempt to characterize the non-variant strain of SARS-CoV-2. As recently seen with the omicron variant, changes in infectivity and severity of infections may be indicative of substantially different shedding rate and infectious dose for a particular variant, hence altering absolute risk and time to infection  $t_{\text{INF}}$ .<sup>108</sup> With respect to vaccines, Riemersma<sup>109</sup> reports shedding rates to be unaffected by vaccination status of infected individuals based on PCR threshold cycle (Ct) data for the SARS-CoV-2 delta variant.

An infection develops when a receptor inhales sufficient PPQ – the process includes (1) inhalation, (2) deposition onto airway surfaces, and (3) accumulation of a “critical mass” of PPQ at epithelial lung cells to initiate an infection. As mentioned previously, Bazant infers over 10 days, CDC suggests 24 hours for accumulation time between identifiable exposure and actual infection, and Johns Hopkins suggests a median SARS-CoV-2 incubation period of 4-6 days.

Inhaled virions may be latent as they retain virulence within the human body, and cumulative exposure contributions should be considered, even if over multiple days. This model characterizes each continuous exposure and may be applied additively over exposure configurations through any appropriate pathogen latency period.

As Watanabe (2010)<sup>110</sup> proposes for SARS (SARS-CoV-1), the exponential dose-response correlates probability of infection,  $P_d$  as a function of pathogen-specific response factor  $k_j$  and dose  $U_{\text{INF}}$ :

$$P_d = 1 - \exp(-U_{\text{INF}}/k_j) \quad [\text{Eq. 26}]$$

Watanabe establishes  $k_{\text{SARS}} = 410 \text{ PPQ}$ , resulting in median infection probability ( $P_d = 0.50$ ), and dose  $U_{\text{INF}} = 284 \text{ PPQ}$  (SARS). Figure 1 in the paper depicts infectious doses for various coronaviruses ranging 80-800 inhaled virions.

For COVID-19, the DHS (updated 18 May 2021)<sup>111</sup> estimates an infectious dose in humans ranging  $0(10^1) - 0(10^3)$ , based on experimental studies of humans exposed to other coronaviruses, animals exposed to SARS-CoV-2, and modeling estimates. Basu (2021)<sup>112</sup> suggest  $U_{\text{INF}} = 0(10^2) \text{ PPQ}$ , up to 300 PPQ.

Sender (2021)<sup>113</sup> states 1-10% of lung/airway cells have the necessary receptors to allow virion entry and infection – either ACE (angiotensin-converting enzyme) or TMPRSS2 (transmembrane protease, serine 2), suggesting  $0(10^1) - 0(10^2)$  virions may be sufficient to trigger an affirmative COVID-19 infection. Considering the high infectivity of COVID-19 and the varied estimates between 10 and 1,000 virions,  $U_{\text{INF}} = 150 \text{ PPQ}$  is selected for COVID-19 in the base case at  $P_d = 0.50$ . This suggests a response factor  $k = 216 \text{ PPQ}$ :

$$P_{d, \text{COVID-19}} = 1 - \exp(-U_{\text{INF, COVID-19}}/216) \quad [\text{Eq. 27}]$$

<sup>107</sup> As previously mentioned, any change to  $U_{\text{INF}}$  should include reconsideration of  $g$ .

<sup>108</sup> See Section 3.8 for discussion of the Airborne Pathogen Mitigation Index (APMI), a proposed metric which normalizes model results to a scale from 0 to 10, depending on the relative infection risk for specific pathogens of interest and indoor air configurations.

<sup>109</sup> <https://www.medrxiv.org/content/10.1101/2021.07.31.21261387v3.full-text>

<sup>110</sup> <https://onlinelibrary.wiley.com/doi/full/10.1111/j.1539-6924.2010.01427.x>

<sup>111</sup> [https://www.dhs.gov/sites/default/files/publications/mqL\\_sars-cov-2\\_-\\_cleared\\_for\\_public\\_release\\_20201221.pdf](https://www.dhs.gov/sites/default/files/publications/mqL_sars-cov-2_-_cleared_for_public_release_20201221.pdf)

<sup>112</sup> <https://www.nature.com/articles/s41598-021-85765-7>

<sup>113</sup> <https://www.pnas.org/content/118/25/e2024815118>



## 2.9 Model Uncertainty, Calibration, Development [\[back to TOC\]](#)

While this model incorporates established virology, aerosol dynamics, transport phenomenon, and aerodynamic principles for pathogen generation, transport, and fate, including infection, meaningful results inherently depend on qualified input parameters. For COVID-19 specifically, the source shedding rate and infectious dose  $U_{INF}$  are selected from broad ranges of published estimates. In addition, the effect of PPQ dilution from source to receptor is addressed by a homogeneous respiratory cone model, a substantial simplification for sources and receptors that are not stationary or breathing in a singular direction - a more refined model, for example, could radially average the respiratory jet around the center axis of the infected source. Furthermore, departures from well-mixed room air rely on lumped factors that are simplified representations of real-world conditions.

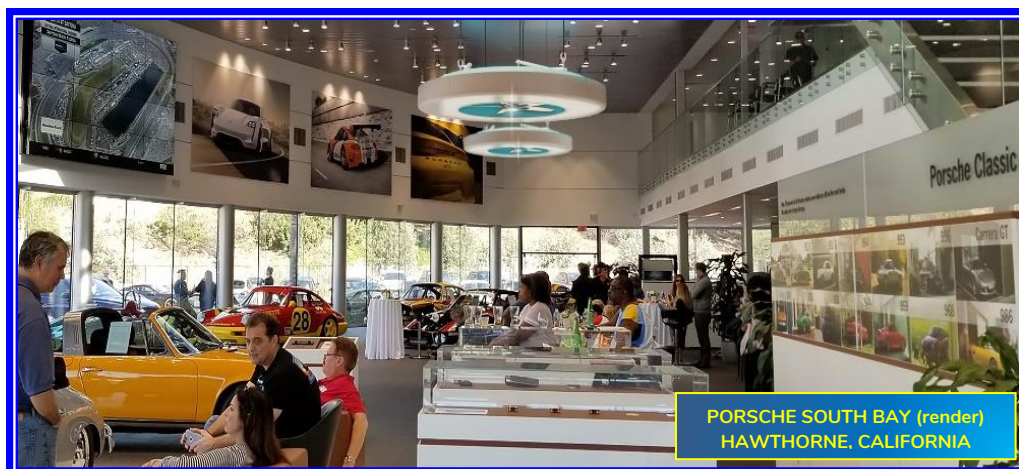
With respect to calibration, Figure 1 depicts a 13% variance from the CDC 15-min guideline. Characterization of respiratory infection risk for common mitigation strategies is presented in the following comparative review and assessment, and results, particularly  $t_{INF}$  and  $\alpha/\beta$ , follow the expected ranking for a variety of mitigation scenarios, including combinations (summarized in Table 3). Further, model results are mostly consistent with Peng (2022) projections for  $t_{INF}$  in various scenarios (see Section 3.8).

Experimental validation of this theoretical model would be of tremendous developmental value. Better analytical and detection techniques should be developed, such as for respiratory jet characterization including proximity and downwind scenarios – perhaps using a refined breathing source with accurate and realistic pulsed respiratory jets/puffs, and a more precise tracer visualization technique with isotopes or detectable dusts.

The model should be further applied to known “superspreader” events for COVID-19 transmission, including the Skagit, Washington choir event of March 2020,<sup>114</sup> and reported outbreaks in long-term care facilities, prisons, etc.<sup>115</sup> Further, a sensitivity analysis should be conducted to determine the relative impact of small and large changes to critical input parameters – for example, parameters that characterize the transport/fate of respiratory jets and PPQ dispersion should be carefully evaluated, as they are primary contributors to short-term exposure risks.

There is evidence that SARS-CoV-2 infectivity and shedding dynamics may differ by variant, as well as for different source/receptor population groups. Input parameters should be reviewed and updated as new information is available, especially if the model is to be used for public policy and epidemiological forecasts or guidance.

Finally, this model is a first-generation attempt to present a unified methodology, based on current knowledge pertaining to respiratory transmission, to characterize infection risk indoors, concurrent with practical usability as simple as entering a few site-specific, “initial condition” parameters in a spreadsheet. Ongoing refinement is essential as new data, studies, analytic tools, and experimental methods become available. With appropriate input parameters, the model can generate probabilistic risk scores for the “healthiness” of indoor air, thereby guiding respiratory transmission mitigation strategies.



<sup>114</sup> <https://www.cdc.gov/mmwr/volumes/69/wr/mm6919e6.htm>

<sup>115</sup> <https://covid19settings.blogspot.com/p/blog-page.html>

### 3 Assessment of Mitigation Strategies [\[back to TOC\]](#)

As depicted in Figure 1, the model establishes a median (50<sup>th</sup> percentile) infection risk for proximate receptors in 17 minutes of continued exposure in the absence of mitigation efforts. Here various strategies are analyzed and ranked (including CADR/ACH comparison and introduction of a new airborne pathogen mitigation index) with base case assumptions plus strategy-specific parameters, including social distancing; masks for receptor(s) and/or source; transparent partitions; ventilation enhancement; HVAC with air treatment/filtration; and, various real-time air disinfection approaches.

Table 3 provides modeling results, along with specific model parameters for mitigation scenarios incorporating specific strategies. The following values were used for all model runs, recapping Table 2:

- Room air volume:  $V = 9,700 \text{ ft}^3$  (10 ft ceiling)
- Initial airborne PPQ:  $N_0 = 0 \text{ PPQ}$
- Number of sources:  $q_{\text{INF}} = 1 \text{ person}$
- Total people:  $p = 30 \text{ pp}$
- Proximal/downwind receptors:  $q_R = 5 \text{ pp}$
- Pathogen shedding rate:  $g = 100 \text{ PPQ/br}$
- Breathing rate:  $n_B = 16 \text{ br/min/pp}$
- PPQ settling fraction:  $s = 0.05$
- PPQ reentrainment fraction:  $r = 0.10$
- PPQ half-life in air:  $t_{1/2} = 66 \text{ min}$
- Exhaust-specific zone factor:  $f_{Z-E} = 1.0$
- Treatment system control efficiency:  $e_T = 0.999$
- Filtration-specific zone factor:  $f_{Z-F} = 1.0$
- Filtration system control efficiency:  $e_F = 0.999$
- Tidal volume:  $\dot{V}_I = 0.016 \text{ ft}^3$
- Inhalation breathing zone factor:  $f_{Z-I} = 1.0$
- Volume correction factor (respiratory jet):  $f_V = 2.0$
- Horizontal respiratory jet velocity:  $v_{H,R} = 71 \text{ ft/min}$
- Respiratory jet cone apex angle:  $\theta_Q = 30^\circ$
- Infectious PPQ dose (COVID-19):  $U_{\text{INF}} = 150 \text{ PPQ}$

**Table 3. Model parameters,  $\alpha/\beta + t_{\text{INF}}$  results for mitigation scenarios (ascending  $t_{\text{INF}}$ ).<sup>a</sup>**

Mitigation Scenario <sup>b</sup>	$f_{M-E}$	$\dot{V}_E$ CFM	$\dot{V}_T$ CFM	$f_{Z-T}$	$\dot{V}_F$ CFM	$f_{M-I}$	$x$ ft	$f_{M-\theta}$	$f_{M-V}$	$v_{H,A}$ ft/min	$\alpha/\beta$ PPQ	$t_{\text{INF}}$ <sup>c</sup> min
Base case (no mitigation)	0	450	0	1.0	0	0	4.5	1.0	1.0	49	25,800	17
2x ventilation from outside	0	<b>900</b>	0	1.0	0	0	4.5	1.0	1.0	49	14,300	18
HVAC + HEPA	0	450	0	1.0	<b>550</b>	0	4.5	1.0	1.0	49	13,000	18
Honeywell HPA 300 purifier (2)	0	450	<b>600</b>	<b>2.5</b>	0	0	4.5	1.0	1.0	49	7,000	18
Healthe Air 2.0 ceiling troffers (4)	0	450	<b>200</b>	1.0	0	0	4.5	<b>1.2</b>	1.0	49	19,200	25
Aerapy Zone 360X ceiling UVGI	0	450	<b>530</b>	1.0	0	0	4.5	<b>1.3</b>	1.0	49	13,400	29
Receptors with masks	0	450	0	1.0	0	<b>0.50</b>	4.5	1.0	1.0	49	26,300	34
Social distancing $\geq 6 \text{ ft}$	0	450	0	1.0	0	0	<b>6.0</b>	1.0	1.0	49	26,200	38
Source with mask	<b>0.50</b>	450	0	1.0	0	0	4.5	<b>4.0</b>	<b>0.25</b>	49	13,000	48
Haiku UV-C 84" ceiling fan	0	450	<b>500<sup>d</sup></b>	1.0	0	0	4.5	1.0	1.0	<b>10</b>	13,900	51
All masks	<b>0.50</b>	450	0	1.0	0	<b>0.50</b>	4.5	<b>4.0</b>	<b>0.25</b>	49	13,200	94
Transparent partitions	0	450	0	1.0	0	0	4.5	<b>4.0</b>	1.0	49	26,500	140
Transparent partitions + all masks	<b>0.50</b>	450	0	1.0	0	<b>0.50</b>	4.5	<b>5.5</b>	<b>0.25</b>	49	13,300	163
Social distancing $\geq 6 \text{ ft}$ + all masks	<b>0.50</b>	450	0	1.0	0	<b>0.50</b>	<b>6.0</b>	<b>4.0</b>	<b>0.25</b>	49	13,300	193
<b>the halo™</b>	0	450	<b>2,000</b>	<b>2.5</b>	0	0	4.5	<b>3.0</b>	1.0	<b>10</b>	<b>2,700</b>	<b>513</b>

<sup>a</sup>  $f_{M-E}$  - exhaled PPQ fraction captured by mask;  $\dot{V}_E$  - volumetric exhaust ventilation airflow;  $\dot{V}_T$  - treatment system volumetric airflow;  $f_{Z-T}$  - treatment-specific zone factor;  $\dot{V}_F$  - filtration system volumetric airflow;  $f_{M-I}$  - inhalation PPQ fraction captured by mask;  $x$  - minimum distance between source/receptors;  $f_{M-\theta}$  - mask/vertical airflow angle expansion factor;  $f_{M-V}$  - mask velocity retardation factor;  $v_{H,A}$  - horizontal bulk air velocity;  $\alpha$  - generation coefficient;  $\beta$  - depletion coefficient;  $U_{\text{PPQ}}$  - cumulative PPQ uptake by a receptor; and,  $t_{\text{INF}}$  - time for receptor to accumulate infectious dose.

<sup>b</sup> For simplicity, it is assumed all treatment and filtration devices (excluding masks) inactivate or capture 99.9% of PPQ in air that flows through them.

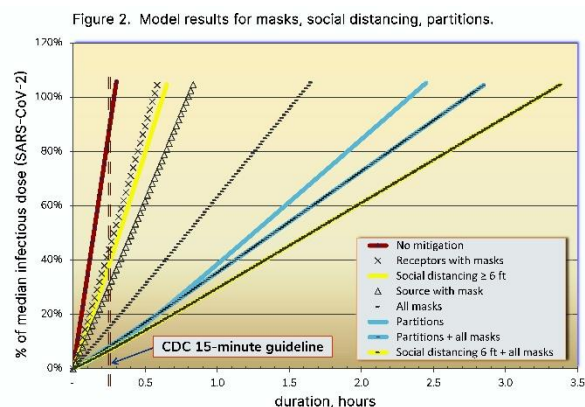
<sup>c</sup> Times to infection are based on parameters specific to non-variant SARS-CoV-2 and will vary for other pathogenic strains. See Section 3.8 for a discussion of the proposed APMI.

<sup>d</sup> The assumed flowrate for the Haiku fan is 2,000 CFM, adjusted by 0.25 because less than 25% of the fan circulating air is actually subject to UV-C disinfection.

### 3.1 Social Distancing, Masks, Partitions [\[back to TOC\]](#)

Model results show that social distancing, masks, and partitions, while often inconvenient or difficult to enforce proper use, can have a significant impact on mitigating short-term exposure risk to PPQ in respiratory jets – extending  $t_{INF}$  from 17 min with no mitigation to over 3 hr with combined distancing and masks for source and receptors. Individually, social distancing or masks provide similar protection. Partitions are the most effective, with  $t_{INF} > 2$  hr as a singular mitigation. Masks worn by an infected source and/or receptors can also reduce the ambient PPQ load and receptor exposure over longer time periods.

Figure 2 depicts social distancing, masks, and partitions in comparison to the base case and CDC 15-min guideline. All three strategies break up respiratory jets and disperse the apex angle, providing a net benefit despite the adverse contribution of retarding respiratory jet forward velocity. Social distancing is effective for reducing the localized PPQ concentration with distance cubed, and masks reduce the PPQ exhaled and/or inhaled in proportion to the mask efficiency.



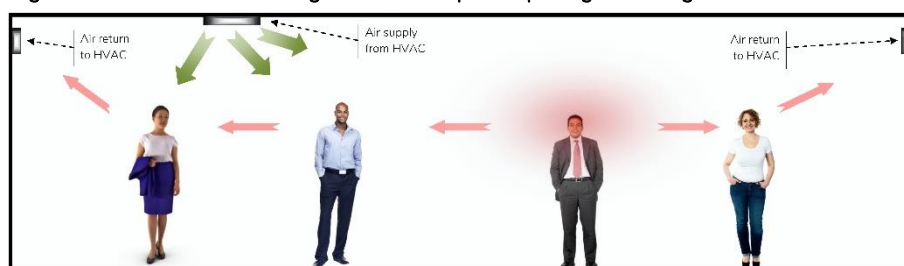
This assessment of masks assumes all are 50% effective at reducing airborne PPQ loadings, either exhaled by sources, or inhaled by receptors. As previously noted, Clapp and Asadi offer FFE measurements with respect to specific face coverings and that N95 respirators do not necessarily provide 95% of reduction in viral shedding/release rates. However, assuming 95% default effectiveness for N95 masks on the same basis for inhalation and exhalation of the PPQ of interest,<sup>116</sup> the model shows:

- Receptors are protected for 5.4 hours when only receptors are wearing N95 masks with  $\alpha/\beta = 26,800$  PPQ. This 10x improvement is consistent with the 10-fold reduction in airborne PPQ load from 50% to 95%.
- Receptors are protected for 7.7 hours when only sources are wearing N95 masks with  $\alpha/\beta = 1,300$  PPQ.
- Receptors are protected for well over 100 hours when all are wearing N95 masks with  $\alpha/\beta = 1,340$  PPQ. This finding is consistent with the well-documented effectiveness of properly used N95 masks for health-care workers, as an example.

### 3.2 Ventilation and Central HVAC [\[back to TOC\]](#)

Atmospheric ventilation exchanges room air with fresh outside makeup air, and may be achieved with open windows or doors, exhaust vents, or central HVAC integration. HVAC removes room air, may filter or treat the air, and returns treated air with makeup

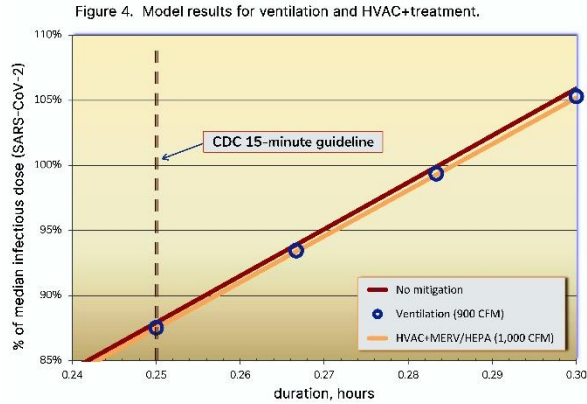
Figure 3. HVAC mixes breathing zone air and spreads pathogens throughout the room.



air. Ventilation and HVAC are important for comfort conditioning, replenishing depleted oxygen, and eliminating allergens and excess carbon dioxide generated by people, although ventilation and HVAC are not effective for reducing localized PPQ concentrations from dispersing respiratory jets.

Return and supply points for ventilation and HVAC may be in the ceiling or walls of a room. Ventilation in the ceiling is commonplace (such as kitchen and bathroom vents). It may not be practical or cost-effective to significantly increase ventilation airflows, due to excess noise or air pollution near highways and industrial areas, security or weather concerns, and increased heating/cooling/conditioning burden.

<sup>116</sup> <https://www.cdc.gov/niosh/nioshtic-2/20023155.html>



HVAC return and supply registers in the walls may be within or above the breathing zone and may cause bulk air flow across the breathing zone resulting in narrowing of respiratory jets, thereby reducing dilution and increasing the localized PPQ concentration for proximal or downwind receptors. Figure 3 depicts general airflow patterns from a ceiling-based ventilation/HVAC system with an infected source in the room. Respiratory jets are not actively dispersed, and local PPQ concentrations may persist if the source remains present.

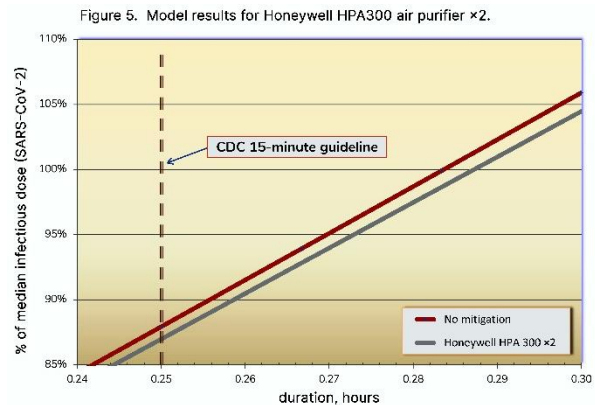
Figure 4 shows model results for 2x ventilation at 900 CFM (6x California Building Code standard for general occupancy) and HVAC recirculation at 550 CFM (in addition to the 450 CFM atmospheric ventilation rate, together achieving 6 air changes/hr)

with 99.9% PPQ treatment/filtration efficacy. While long term steady-state PPQ concentrations are significantly reduced, the short-term impact of respiratory jet exposure is essentially equivalent to no mitigation.

### 3.3 Portable Air Purifiers [\[back to TOC\]](#)

Portable air purifiers and cleaning devices typically include a fan and method to filter or treat the air, including HEPA and MERV filters, ionization, chemicals, radio-frequency waves, ozone, activated carbon, or germicidal UVC lights. A top-rated product is the Honeywell HPA300 HEPA large room air purifier.<sup>117</sup> Specifications for this unit include up to 465 ft<sup>2</sup> coverage area and CADR ~300 CFM.

Using two HPA300 units with the infectious dose model, setting  $\dot{V}_T = 600$  CFM and  $f_{Z-T} = 2.5$  (on the floor or table-top, assumed to be treating air from the breathing zone, estimated to represent ~40% of total room air), Figure 5 depicts the performance of the HPA300 or similar units relative to the no mitigation baseline and CDC guideline. Portable air purifiers are not designed to break up respiratory jets or control the breathing zone, hence short-term results are similar to the no mitigation base case, although a significantly reduced  $\alpha/\beta$  ratio is indicative of lower long term, steady-state PPQ concentrations.



### 3.4 Ceiling-Based Systems (Troffers, Upper-Room UVGI and Ceiling Fans) [\[back to TOC\]](#)

Ceiling-based systems, such as troffers, ceiling fans,<sup>118</sup> and other upper air disinfection units including are used to disinfect upper room air. Disinfection may be provided by filtration, ionization, chemicals, radio-frequency waves, ozone, activated carbon, or germicidal UVC or UVGI<sup>119</sup> lights of various wavelengths and bulb types. Figure 6 includes model results for Healthe Air 2.0 ceiling troffers ( $\dot{V}_T = 50$  CFM x 4 units = 200 CFM),<sup>120</sup> Aerapy Zone360X upper-room UVGI unit ( $\dot{V}_T = 530$  CFM),<sup>121</sup> and Haiku UV-C 84" ceiling fan ( $\dot{V}_T = 500$  CFM – 25% of assumed fan airflow).<sup>122</sup>

Low airflows into the troffers and upper-room UVGI unit are insufficient to effectively control breathing zone air, although they both draw air up towards the ceiling. The model estimates this with mask/vertical airflow angle expansion factor  $f_{M-\theta} = 1.2$  for Healthe and  $f_{M-\theta} = 1.3$  for Aerapy.

<sup>117</sup> <https://www.bestreviews.guide/cadr-rated-air-purifiers?>

<sup>118</sup> Commercial ceiling fans with disinfection are used in downflow mode.

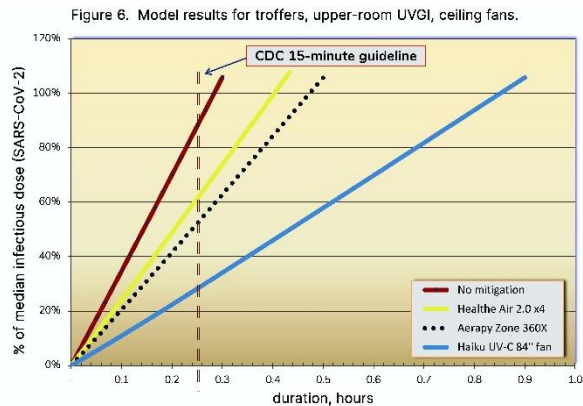
<sup>119</sup> UV germicidal irradiation.

<sup>120</sup> [https://healtheinc.com/app/media/2020/11/Healthe\\_Air2.0\\_SpecSheet\\_v15.pdf](https://healtheinc.com/app/media/2020/11/Healthe_Air2.0_SpecSheet_v15.pdf)

<sup>121</sup> <https://aerapy.com/upper-air-uv/zone360x/>

<sup>122</sup> <https://www.cleanairsystem.com/technology/?section=uv-c-technology>

The angle correction does not apply to a downflow ceiling fan, as the respiratory jet angle is not expanded upward. The fan does, however, significantly reduce any lateral air currents. The model estimates this benefit with horizontal bulk air velocity  $V_{HA} = 10$  ft/min, an 80% reduction from the base case.



exhaled breath into vertical currents, with corresponding quick dispersion/dilution of PPQ and improvement in  $t_{INF}$  to 49 minutes with a 2,000 cfm downflow fan (breezy), and 176 minutes for a 2,000 cfm upflow fan (almost imperceptible), in spite of no substantive change in  $\alpha/\beta$ . Hence, running a simple ceiling fan, preferably in reverse or upflow mode, can provide limited short-term protection from respiratory infection.

With respect to ceiling fans,  $f_{M-V}$  is similarly corrected for both upflow and downflow fans because any vertical bulk air flow reduces the lateral extent of exhaled jets over the breathing time scale. However,  $f_{M-\theta}$  is not necessarily increased for downflow fans because the "cone of influence" is substantially narrower than for an upflow fan. The downflow scenario is highly dependent on the location of a shedding individual relative to the ceiling fan (separate consideration could be given to the "fumigation" phenomenon as the downflow jet impinges on the floor or other surfaces). As the main objective of  $f_{M-\theta}$  is to characterize the vertical dispersion of respiratory jets in a reasonable worst-case, the present study conservatively assumes  $f_{M-\theta} = 1.0$  for downflow fans – a more refined approach could involve consideration of the proportional area covered by the downward cone.

### 3.5 the halō: A Viable Alternative (Encapsulated Low-UVC Active Disinfection) [\[back to TOC\]](#)

Reviewed methods for indoor air disinfection have various limitations that make them ineffective for preventing respiratory transmission for much more than an hour or with regular potential exposure. **the halō**, a ceiling-based system in the center of a room incorporates an upflow ceiling fan combined with an encapsulated low-wavelength germicidal UVC (low-UVC) light ring. **the halō**, depicted on the cover page, effectively addresses ventilation and disinfection limitations of current approaches by combining three unique design elements:

- **Breathing Zone Control** - Effective capture of exhaled air with an upflow fan, within seconds and from the middle of the ceiling – designed with the ideal location especially due to natural warm loft of exhaled breath and based on a measured "cone of influence" in the breathing zone of a room, with linear air velocities towards **the halō** that are gentle yet effective to capture respiratory aerosols and redirect respiratory jets.
- **Proven Disinfection** - Effective inactivation of airborne pathogens in a low-UVC light ring, specifically proven in commissioned Boston University Medical School exposure trials to kill 99.9% of the COVID-19 virus and designed to deliver the optimal disinfecting low-UVC dose.
- **Directional Airflow** - Effective flow patterns for indoor room air with an aerodynamic cowl system - designed to maximize clean air flow back into the breathing zone, disperse respiratory jets as with masks and partitions, and minimize the mixing of treated and untreated air.

Figure 7 provides model results for **the halō**, and comparison to other measures including social distancing with masks (next-best of all options), Haiku ceiling fan (best of the ceiling-based alternatives), and HVAC in-duct air treatment. The model suggests remarkable performance for **the halō**, extending  $t_{INF}$ :

- 10x+ better than any disinfection alternative;



- 3x better than social distancing plus masks; and,
- >40x better than the no mitigation base case.

Four key model parameters contribute to this result:  $\dot{V}_T = 2,000$  CFM with a 60" fan,  $f_{Z-T} = 2.5$  (all the air entering the halō is from the breathing zone),  $f_{M-0} = 3.0$  (upflow extends the respiratory jet dispersion angle); and,  $v_{H,A} = 10$  ft/min (80% reduction from base case as horizontal ambient currents are substantially redirected to the vertical).

Due to breathing zone control, directional airflow, and rapid and thorough disinfection of substantial airflow in a 1,000 ft<sup>2</sup> room, normal operation of **the halō** achieves over **30 ACH<sub>e</sub>**. For context, this is double the CDC minimum ACH standard for the most sensitive medical areas:

- USEPA: Recommends a design minimum of 0.35 ACH for residences;<sup>123</sup>
- ASHRAE: For commercial and public spaces, Table 6.4 of the 2003 standard, *Ventilation for Acceptable Indoor Air Quality Addendum n*,<sup>124</sup> minimum exhaust rates range from 0.25 to 1.50 CFM/ft<sup>2</sup>. Assuming 10 ft ceilings, this represents a range of 1.5-9.0 ACH; and,
- CDC: For health care facilities, Table B.2 in the reference<sup>125</sup> requires 15 ACH for critical occupied areas such as surgical and delivery rooms.

ACH, CADR, and ACH<sub>e</sub> are further discussed in [Section 3.7](#).

### 3.6 Entering an Infectious Space (No Continuous Source) [\[back to TOC\]](#)

In the no mitigation scenario, the continuous source results in steady-state, well-mixed PPQ loading of 25,800 PPQ ( $= \alpha/\beta$ ) in the aggregate room air based on an assumed pathogen shedding rate per breath  $g$  from one infected source. If the source leaves the room at  $t = 0$  with initial loading  $N_0 = 25,800$  PPQ and no further settling ( $s = 0$ ), the respiratory jet can be neglected, the well-mixed condition requires no zone-specific adjustments, and source mask, social distancing, and partitions are not relevant (receptor masks are still considered). With no continuing source,  $\alpha = 0$  and Equation 23 becomes a simple exponential decay function for active PPQ:

$$\begin{aligned} N(t) &= [N_0 - (\alpha/\beta)]e^{-\beta t} + (\alpha/\beta) \\ &= N_0 e^{-\beta t} \end{aligned}$$

The effective half-life  $T_{50}$ , or time for 50% active PPQ depletion via exhaust/ventilation, treatment, filtration, natural decay, and inhalation, is:

$$\begin{aligned} T_{50} &= - (1/\beta) \cdot \ln[(N(t)/N_0)] \\ &= (\ln 2)/\beta \end{aligned}$$

The following base values were used for all alternative model runs (asterisks denote values that are the same as for the continuing source base case, although they are not material to a no continuing source scenario):

- Room air volume:  $V = 9,700$  ft<sup>3</sup> (10 ft ceiling)
- Initial airborne PPQ:  $N_0 = 25,800$  PPQ
- Number of sources:  $q_{INF} = 0$  persons
- Total people:  $p = 30$  pp
- Proximal/downwind receptors:  $q_R = 0$  pp
- Pathogen shedding rate:  $g = 0$  PPQ/br

Figure 7. Model results for the halō and comparison.

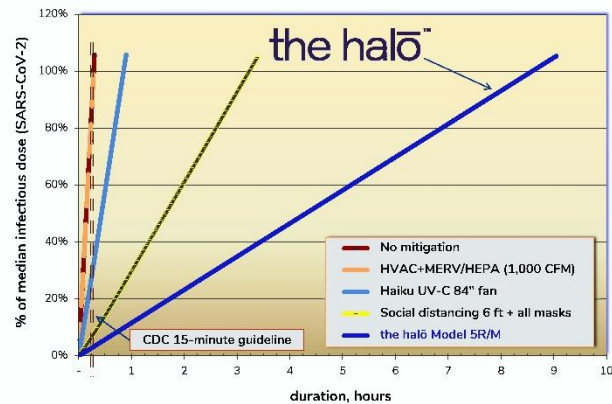
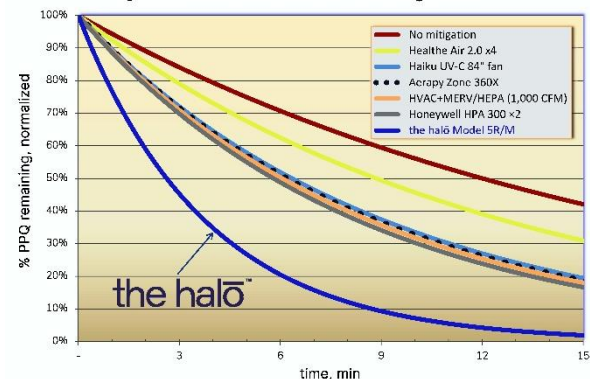


Figure 8. Model results with no continuing source.



<sup>123</sup> <https://www.epa.gov/indoor-air-quality-iaq/how-much-ventilation-do-i-need-my-home-improve-indoor-air-quality>

<sup>124</sup> [https://www.ashrae.org/File%20Library/Technical%20Resources/Standards%20and%20Guidelines/Standards%20Addenda/62-2001/62-2001\\_Addendum-n.pdf](https://www.ashrae.org/File%20Library/Technical%20Resources/Standards%20and%20Guidelines/Standards%20Addenda/62-2001/62-2001_Addendum-n.pdf)

<sup>125</sup> <https://www.cdc.gov/infectioncontrol/guidelines/environmental/appendix/air.html#tableb2>

- Breathing rate:  $n_B = 16$  br/min/pp
- Exhaled PPQ fraction captured by mask:  $f_{M-E} = 0$  \*
- PPQ settling fraction:  $s = 0$
- PPQ reentrainment fraction:  $r = 0.10$
- PPQ half-life in air:  $t_{1/2} = 66$  min (natural decay only)
- Exhaust-specific zone factor:  $f_{Z-E} = 1.0$  \*
- Treatment-specific zone factor  $f_{Z-T} = 1.0$  \*
- Treatment system control efficiency:  $e_T = 0.999$
- Filtration-specific zone factor:  $f_{Z-F} = 1.0$  \*
- Filtration system control efficiency:  $e_F = 0.999$
- Tidal volume:  $\dot{V}_I = 0.016$  ft<sup>3</sup>
- Inhalation PPQ fraction captured by mask:  $f_{M-I} = 0$  \*
- Inhalation breathing zone factor:  $f_{Z-I} = 1.0$  \*
- Volume correction factor (respiratory jet):  $f_V = 2.0$  \*
- Minimum distance between source/receptors  $x = 4.5$  ft \*
- Mask/vertical airflow angle expansion factor  $f_{M-\theta} = 1.0$  \*
- Mask velocity retardation factor  $f_{M-v} = 1.0$  \*
- Horizontal respiratory jet velocity:  $v_{H,R} = 71$  ft/min \*
- Horizontal bulk air velocity  $v_{H,A} = 49$  ft/min \*
- Respiratory jet cone apex angle:  $\theta_Q = 30^\circ$  \*
- Generation coefficient:  $\alpha = 0$

**Table 4. Alternative model parameters (initial PPQ load, no continuing source, ascending  $\beta$ /descending  $T_{50}$ ). \***

Mitigation Scenario **	$\dot{V}_E$ CFM	$\dot{V}_T$ CFM	$\dot{V}_F$ CFM	$\beta$ min <sup>-1</sup>	$T_{50}$ min
Alternative base case (no mitigation)	450	0	0	0.058	12
Health Air 2.0 ceiling troffers (4)	450	200	0	0.078	8.8
2x ventilation from outside	900	0	0	0.10	6.6
Haiku UV-C 84" ceiling fan	450	500 ***	0	0.11	6.4
Aerapy Zone 360X ceiling UVGI	450	530	0	0.11	6.1
HVAC + HEPA	450	0	550	0.11	6.0
Honeywell HPA 300 purifier (2)	450	600	0	0.12	5.8
<b>the halō™</b>	450	2,000	0	0.26	2.6

\*  $\dot{V}_E$  - volumetric exhaust ventilation airflow;  $\dot{V}_T$  - treatment system volumetric airflow;  $\dot{V}_F$  - filtration system volumetric airflow;  $f_{M-I}$  - inhalation PPQ fraction captured by mask;  $\beta$  - depletion coefficient; and,  $T_{50}$  - time for 50% airborne PPQ to be depleted or inactivated.

\*\* For simplicity, it is assumed all treatment and filtration devices (excluding masks) inactivate or capture 99.9% of PPQ in air that flows through them.

\*\*\* The assumed flowrate for the Haiku fan is 2,000 CFM, adjusted by 0.25 because less than 25% of the fan circulating air is actually subject to UV-C disinfection.

Figure 8 depicts results graphically with PPQ reduction over time for selected mitigation scenarios; Table 4 provides modeling results for the no continuing source alternative, along with specific model parameters each mitigation strategy.

As for the base case with a continuing source, the halō performs remarkably better than other mitigation strategies: Air cleared of pathogens >4x faster than no mitigation and >2x faster than any other option. As expected, the time for air disinfection is inversely proportional to the combined rate of clean air returned to the room from ventilation, treatment, and filtration systems (including NDOs).

The earlier base case demonstrates the significance of respiratory jets and importance of breaking or dispersing jets, including masks, social distancing, and partitions. This alternative case additionally shows the critical role of ventilation, treatment, and filtration flowrates to affect a greater depletion rate.

### 3.7 Comparison to ACH and CADR [\[back to TOC\]](#)

Common HVAC industry terms for characterizing ventilation rates include CADR and ACH. CADR represents the ventilation air flowrate (volume/unit time), and ACH is the ratio of hourly CADR to the air volume of an indoor space. Hence  $CADR = \dot{V}_E$  (CFM) and:

$$ACH = 60 \bullet CADR/V = 60 \bullet \dot{V}_E/V \quad [\text{Eq. 30}]$$

CADR and ACH are calculated for bulk ventilation (well-mixed assumption), and do not account for localized airborne PPQ concentrations or PPQ filtration and treatment. CADR and ACH are not affected by masks, social distancing, or partitions. Divergence from well-mixed conditions and PPQ filtration/treatment are incorporated with equivalent ACH ( $ACH_e$ ), as previously discussed:

$$ACH_e = (60/V) \bullet (\dot{V}_E f_{Z-E} + e_T \dot{V}_T f_{Z-T} + e_F \dot{V}_F f_{Z-F} + p \dot{V}_I f_{Z-I}) \quad [\text{Eq. 31}]$$

The depletion coefficient  $\beta$  is defined in Eq. 22:

$$\beta = (1/V) [\dot{V}_E f_{Z-E} + e_T \dot{V}_T f_{Z-T} + e_F \dot{V}_F f_{Z-F} + (V/t_{1/2})(\ln 2) + (1 - f_{M-I})(p - q_R) \dot{V}_I n_B f_{Z-I}]$$

$ACH_e$  and  $\beta$  are similar except for natural decay and inhaled PPQ adjustments in  $\beta$ . Both adjustments are expected to be small in magnitude relative to exhaust/ventilation, treatment, and filtration terms:<sup>126</sup>

$$ACH_e \gg p \dot{V}_{fz-i}$$

$$\beta \gg (1/V)[(V/t_{1/2})(\ln 2) + (1 - f_{M-i})(p - q_R)\dot{V}_{inBfZ-i}]$$

hence

$$ACH_e \sim 60 \cdot \beta$$

For the ventilation, treatment, and filtration strategies under consideration herein,  $ACH_e$  and  $\beta$  are tabulated in Table 5, with  $ACH_e$  depicted in Figure 9. The  $ACH_e/(60\beta)$  ratio ranges from 0.81 for the base case (nominal ACH at 2.8) up to 0.98 for the halō.

Table 5. Comparison of  $ACH_e$ ,  $\beta$ , and APMI

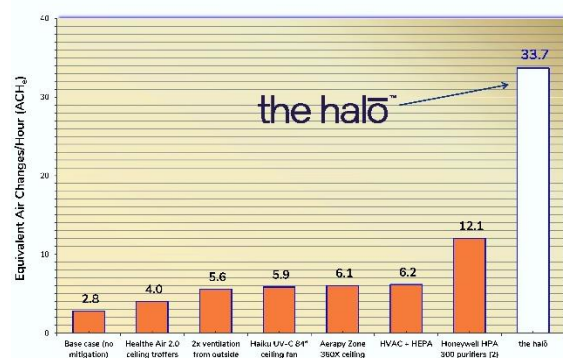
Mitigation Scenario **	$\beta$ min <sup>-1</sup>	$ACH_e$ hr <sup>-1</sup>	$ACH_e/$ (60 • $\beta$ )	APMI
Base case (no mitigation)	0.058	2.8	0.81	0.037
Health Air 2.0 ceiling troffers (4)	0.078	4.0	0.86	.019
2x ventilation from outside	0.10	5.6	0.89	0.056
Haiku UV-C 84" ceiling fan	0.11	5.9	0.90	0.68
Aerapy Zone 360X ceiling UVGI	0.11	6.1	0.90	0.26
HVAC + HEPA	0.11	6.2	0.90	0.056
Honeywell HPA 300 purifiers (2)	0.21	12	0.95	0.056
the halō™	0.57	34	0.98	9.4

Regulatory and best practice ACH standards range widely by use case and associated respiratory infection risk:

- USEPA recommends at least 0.35 ACH for residences;<sup>127</sup>
- ASHRAE establishes standards for commercial and public spaces in Table 6.4 of the 2003 ASHRAE standard 62-2001, *Ventilation for Acceptable Indoor Air Quality Addendum n*.<sup>128</sup> Minimum exhaust rates range 0.25 to 1.50 CFM/ft<sup>2</sup>, and with 10 ft ceilings this represents a range of 1.5-9.0 ACH;
- 2018 ASHRAE standard 170-2017, *Ventilation for Health Care Facilities Addendum n*,<sup>129</sup> provides minimum total ACH up to 12 for emergency waiting rooms, anterooms, and medical waste holding spaces;
- CDC requires 15 ACH for health care facilities per Table B.2<sup>130</sup> in critical occupied areas such as surgical and delivery rooms; and,
- Subhash<sup>131</sup> provides an overview of ACH guidelines and standards for isolation anterooms and the critical components of airborne infection control.

This  $ACH_e$  analysis reinforces the importance of effective air treatment and breaking/dispersing respiratory jets, breathing zone control, a substantial volumetric air flow rate through the treatment system, and directional airflow to minimize mixing of treated and untreated air. For example, two portable Honeywell HPA 300 purifiers provide a high ACH rate, yet Table 3 and Figure 5 illustrate

Figure 9.  $ACH_e$  for ventilation, treatment, and filtration strategies.



$t_{INF}$  is only around 18 minutes, with respiratory infection risk substantially the same as no mitigation – this is because two portable air purifiers are not sufficient to clear the breathing zone, provide directional airflow, or disperse respiratory jets in a room occupied by 30 people. The short-term exposure risk is not mitigated.

ACH rates over 10 are often specified for indoor locations with a high risk of potential respiratory infection - which, as the COVID-19 pandemic has clearly illustrated, could be almost any public place where people gather and remain in close contact (< 6 feet) for over 15 minutes. However, as depicted in Table 3, Table 5 and Figure 4,  $ACH_e$  for HVAC with treatment is over twice the base case, yet  $t_{INF}$  is only marginally (6 percent) better. Increasing  $ACH_e$  is not

sufficient to reduce the airborne infection risk, as it does not guarantee control of the breathing zone and mitigation of respiratory jets.

<sup>126</sup> This is not valid for pathogens with short half-lives; specific to SARS-CoV-2 with a half-life of 66 min, the natural decay term ( $V \ln 2/t_{1/2}$ ) is 102, which increases inversely with half-life.

<sup>127</sup> <https://www.epa.gov/indoor-air-quality-iaq/how-much-ventilation-do-i-need-my-home-improve-indoor-air-quality>

<sup>128</sup> [https://www.ashrae.org/File%20Library/Technical%20Resources/Standards%20and%20Guidelines/Standards%20Addenda/62-2001/62-2001\\_Addendum-n.pdf](https://www.ashrae.org/File%20Library/Technical%20Resources/Standards%20and%20Guidelines/Standards%20Addenda/62-2001/62-2001_Addendum-n.pdf)

<sup>129</sup> [https://www.ashrae.org/file%20library/technical%20resources/standards%20and%20guidelines/standards%20addenda/170-2017/170\\_2017\\_n\\_20200303.pdf](https://www.ashrae.org/file%20library/technical%20resources/standards%20and%20guidelines/standards%20addenda/170-2017/170_2017_n_20200303.pdf)

<sup>130</sup> <https://www.cdc.gov/infectioncontrol/guidelines/environmental/appendix/air.html#tableb2>

<sup>131</sup> <https://www.ncbi.nlm.nih.gov/pmc/articles/PMC7135637/>

Furthermore, as discussed in Section 4.6, achieving higher ACH solely by increasing ventilation via fresh outside air is an energy-intensive, costly endeavor with significant carbon footprint ramifications. Effective and rapid treatment of indoor air with breathing zone control and dispersion of respiratory jets is an efficacious, sustainable, and cost-effective alternative to ventilation- and HVAC-based methods to increase ACH.

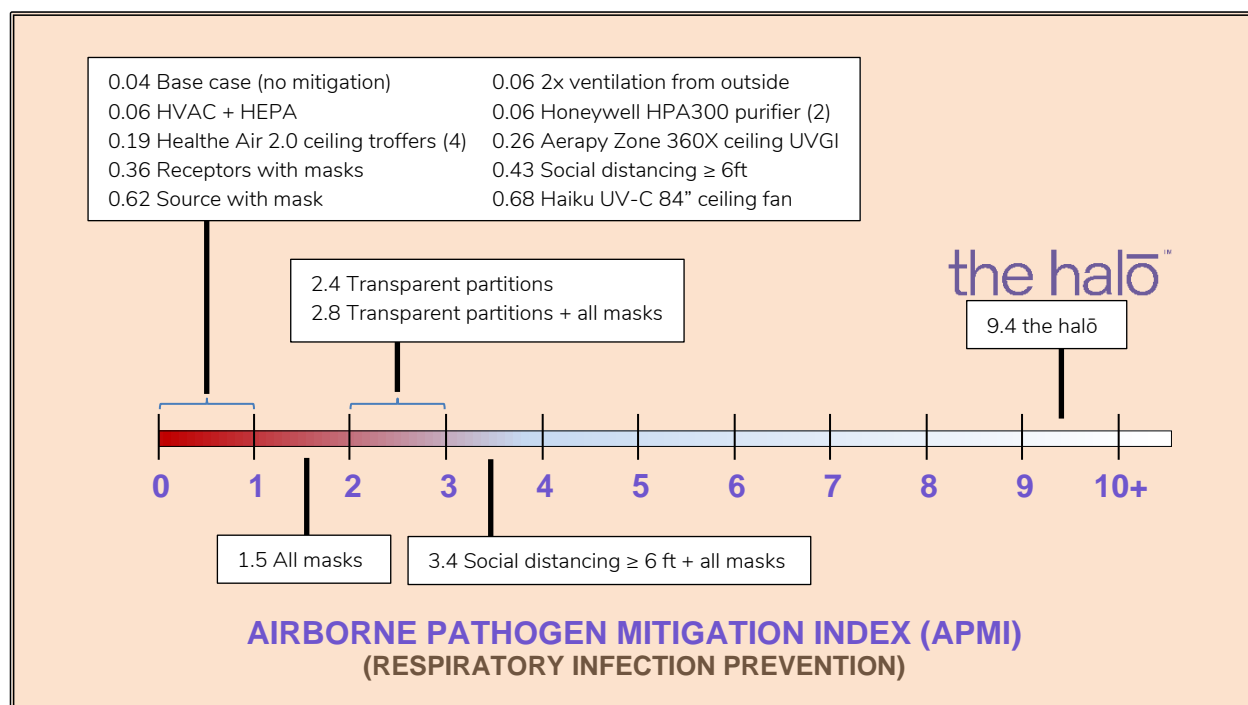
### 3.8 Airborne Pathogen Mitigation Index (APMI) [\[back to TOC\]](#)

While ACH,  $ACH_e$ , and  $\beta$  are useful to characterize airborne pathogen mitigation strategies, they are not linear with the time to infection,  $t_{INF}$  because of varying source/sink significance to the overall pathogen balance. To better inform the public and guide facility managers about the respiratory infection health risk in buildings, a more practical and actionable metric is correlated with  $t_{INF}$ . In addition to site-specific indoor air conditions and occupant behavior,  $t_{INF}$  is highly dependent on the infectivity of a specific pathogen of interest.

Hence it is useful to define a linear, non-dimensional parameter, proposed herein as the Airborne Pathogen Mitigation Index (APMI)<sup>132</sup> to characterize the relative airborne infection risk in a particular indoor setting. Various indoor air quality indices have been proposed by others including Breeze Technologies<sup>133</sup> and Berkeley Lab<sup>134</sup> – these approaches focus on indoor carbon dioxide, contaminants of concern (chemicals or non-pathogen particles), and comfort factors such as odors and humidity. Currently, there is no established index that evaluates the potential airborne infection risk for an indoor space.

The normalized APMI ranges from 0 to 10, with 0 representing the least protection (e.g., no mitigation with  $ACH_e = 2.8$ ) and 10 representing the highest protection from cross-transmission risk of respiratory infection. Because infection risk is determined by both the dose delivery rate (e.g., PPQ intake per breath) and exposure time, the APMI is calibrated from the base case with short-term exposure ~ 15 min (CDC 15-min close contact standard) to full day exposure (8+ hours).

Figure 10. APMI for considered mitigation approaches (continuous source).



<sup>132</sup> Previously known as the Air Protection Index or API.

<sup>133</sup> [https://www.breeze-technologies.de/blog/calculating-an-actionable-indoor-air-quality-index/#~:text=An%20air%20quality%20index%20\(AQI,pollution%20in%20short%20time%20frames.&text=Concentrations%20of%20some%20air%20pollutants,times%20higher%20indoors%20than%20outdoors](https://www.breeze-technologies.de/blog/calculating-an-actionable-indoor-air-quality-index/#~:text=An%20air%20quality%20index%20(AQI,pollution%20in%20short%20time%20frames.&text=Concentrations%20of%20some%20air%20pollutants,times%20higher%20indoors%20than%20outdoors)

<sup>134</sup> <https://svach.lbl.gov/iaq-index-scores-indoor-air-quality/>

To allow for a 13% model departure from the CDC guideline (Section 2.9), APMI is calculated as follows:

$$\text{APMI} = [1.13 \bullet (t_{\text{INF}}/60)] - 0.283 \quad [\text{Eq. 33}]$$

Hence APMI is correlated with  $t_{\text{INF}}$  for the base case and non-variant SARS-CoV-2. Table 5 provides calculated APMI values for selected mitigation scenarios, and Figure 10 depicts APMI for the various scenarios.

For other pathogens, APMI is a strictly a relative comparative index and not an indication of time to/risk of infection. Actual results will vary based on the specific activities of occupants in the room, the number of infected individuals, other variances from modeled conditions, and the pathogen of interest.

Peng (2022) recently proposed a risk parameter,  $H$  ( $\text{pp h}^2 \text{ m}^{-3}$ ), as an approximate indicator of the absolute probability of infection. Considering  $H = 0.05 \text{ pp h}^2 \text{ m}^{-3}$  as a threshold for significant risk of outbreak, Table 2(b) of the reference provides exposure times ( $t_{\text{INF}}$ ) corresponding to  $H$  for various occupancy, face covering, and ventilation scenarios. Table 6 compares derived Peng APMI values for  $t_{\text{INF}}$  as listed in Table 2(b) thereof, and APMI calculated from the model herein for comparable scenarios. There are significant differences between the two models, particularly with respect to the ratio of PPQ infectious dose  $U_{\text{INF}}$  and shedding rate  $g$  – Peng incorporates a relative shedding factor ranging from 1.0 for resting to over 200 for loud speaking with heavy exercise.

Table 6. APMI and risk parameter ( $H$ ,  $\text{pp h}^2 \text{ m}^{-3}$ ) from Peng (2022). \*

Scenario	Peng Model		This Model	
	$t_{\text{INF}}$ hr	Projected APMI	Comparable Scenario	APMI
Poorly ventilated	0.086-0.43	0-0.20	Base case (with $\geq 6$ ft distancing)	0.20
Poorly ventilated + masks	0.24-1.22	0-1.1	Base case + masks	3.6
Well-ventilated	0.51-2.6	0.29-2.7	HVAC + HEPA	0.45
Well-ventilated + masks	1.5-7.3	1.4-8.0	HVAC + HEPA + masks	3.8

\* All scenarios assume  $\geq 6$  ft social distancing between occupants. Exposure times are extracted from Table 2(b) of the Peng reference (<https://pubs.acs.org/doi/10.1021/acs.est.1c06531?ref=pdf>), which provides maximum time until risk of outbreak or  $t_{\text{INF}}$  with  $H = 0.05 \text{ pp h}^2 \text{ m}^{-3}$ . Values compared here are for high occupancy indoor conditions and occupants silent or speaking. Peng includes an online calculator tool at <https://tinyurl.com/covid-estimator> with numerical assumptions. This model assumes 50% mask filtration efficiency for inhaled or exhaled PPQ, whereas Peng assumes 50% for exhalation and 30% for inhalation. Peng assumes a breathing rate of  $0.52 \text{ m}^3/\text{hr}$  in comparison to this model which assumes  $0.44 \text{ m}^3/\text{hr}$  ( $0.5 \text{ L}/\text{br}$  and  $16 \text{ br}/\text{min}$ ). With respect to shedding rate and infectious dose, Peng uses an infectious “quanta” exhalation rate of 18.6 infectious doses/hr for resting, and 87 infectious doses/hr for normal speaking. For comparison, this model base case assumes a PPQ generation rate of 100 PPQ/br and 16 br/min. The infectious dose considered herein is 150 PPQ (Section 2.8.8), so the equivalent “quanta exhalation rate” is  $(100 \text{ PPQ}/\text{br})(16 \text{ br}/\text{min})(60 \text{ min}/\text{hr})/(150 \text{ PPQ}/\text{infection}) = 640 \text{ infectious doses}/\text{hr}$ , or  $> 30\times$  greater than Peng.





#### 4 the halō – Air Disinfection with Breathing Zone Control [\[back to TOC\]](#)

the halō achieves unparalleled air disinfection with effective, directional airflow and disinfection. An upflow ceiling fan gently and quickly carries a high volume of potentially infectious air up and away from the breathing zone as respiratory jets are dispersed,



Figure 11. Expanded view of the halō.

disinfects the air within an encapsulated low-UVC light ring surrounding the fan, and returns disinfected air back to the breathing zone with minimal mixing of treated and untreated air.

the halō is positioned at typical ceiling height in the center of an indoor space (8-12 ft high), and upflow to the ceiling is the most effective method and positioning to control the breathing zone and prevent mixing of treated and untreated air.

Figure 11 depicts main components of the halō, including an upflow ceiling fan, low-UVC light ring encapsulated in a duct-like cowling system, and support triangle. The fan actively disperses respiratory jets as people breathe, hence reducing potential localized PPQ hot spots, enhanced with modulation programming to destabilize undesirable recirculation zones. The proprietary low-UVC light ring delivers the optimal disinfection dose to air flowing through the cowlings to achieve 99.9% inactivation of SARS-CoV-2, influenza strains, and most other respiratory pathogens.

Modeling results demonstrate the importance of dispersing respiratory jets as well as high volumetric airflow with disinfection. the halō is designed to capitalize on the critical parameters necessary to lower airborne PPQ loadings as safely, quickly, and effectively as possible. The following overview describes key design elements including airflow, low-UVC

active disinfection technology, and virology, spectroscopy, and residence time.

##### 4.1 Airflow [\[back to TOC\]](#)

The breathing zone in a room is the volume of air from the floor to a height of 6 ft. In general, this is a contiguous space volume where people may be present, standing, walking, sitting, or lying down. From a point directly above the lateral center of the breathing zone, (7-12 ft above the floor), the halō's upflow flow fan achieves a "cone of influence" that extends down up to 8 ft below the fan and radially outward up to 8 ft from the fan center. This cone of influence is defined as the air volume where the upward velocity of air being induced towards the fan is 0.5-1.0 ft/sec. This is a gentle velocity that occupants of the room experience as a virtually unnoticeable breeze. Figure 12 illustrates typical airflow patterns with an upflow fan.

The airflow needed to achieve this large cone of influence is substantial, in the range of 2,000 CFM. This volumetric flow is readily achieved by a typical ceiling fan operating at 50-70% of capacity, and results in rapid disinfection of the entire breathing zone volume of a 10,000 ft<sup>3</sup> room in a few minutes and much faster than any practical alternative (Figure 8).

the halō incorporates a proprietary fan speed modulation algorithm to destabilize recirculation zones, which can be problematic in terms of effective capture of breathing zone air. By eliminating standing waves and providing robust airflow through the low-UVC light ring, the halō minimizes mixing of untreated air from the breathing zone with treated air from the halō. Modulation includes a startup protocol and ongoing fan speed oscillation.

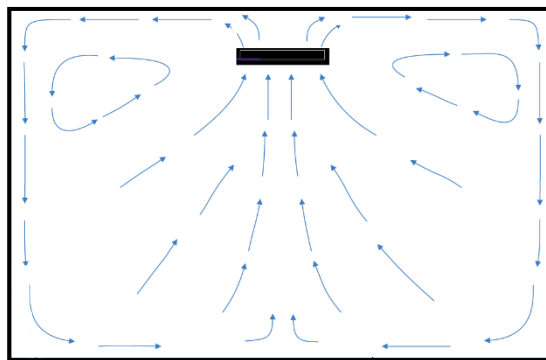


Figure 12. Upflow fan airflow patterns (sans modulation).

In addition to disinfecting a robust volume of breathing zone air with an additional 30 ACH<sub>e</sub>, the halō disperses respiratory jets to mitigate proximate and downwind exposures. These features are quantified in the unified dose model with:

- Treatment-specific zone factor  $f_{z-T} = 2.5$ : Air captured by the halō is exclusively from the potentially infectious portion of the breathing zone at 3-7 ft from the floor, which represents 40% ( $= 1/2.5$ ) of the total room air volume;
- Mask/vertical airflow angle expansion factor  $f_{M-\theta} = 3.0$ : the halō creates upward dispersion of respiratory jets, as with masks and partitions. This factor increases the default quiescent respiratory jet apex angle  $\theta$  from 30° to 90°; and,

- Horizontal bulk air velocity  $v_{HA} = 10$  ft/min: **the halō** creates upward dispersion of bulk lateral air currents as well, conservatively calculated to decrease the effective lateral bulk velocity ~5x.

#### 4.2 Encapsulated Low-UVC Active Disinfection [\[back to TOC\]](#)

All breathing zone air captured by the **halō** fan is directed into the surrounding low-UVC light ring, encapsulated within a cowling system to minimize stray ambient low-UVC reflections. Within the cowling system, nine 254 nm fluorescent bulbs and associated reflectors provide the necessary low-UVC exposure to disinfect PPQ contained in the flowing air. As air swirls axially through the cowling system, internal mixing ensures a uniform low-UVC dose.

Relevant design parameters for the disinfection process include:

- Virology - the susceptibility of specific PPQ to low-UVC and dose needed for a desired inactivation/kill rate of 99.9%/pass;
- Spectroscopy – spatial characterization of low-UVC energy in and around **the halō** to determine optimal disinfection zone geometry within aerodynamic constraints, and to verify ambient levels are below health-based exposure limits; and,
- Residence time – for a given air flowrate and target disinfection dose, the required residence time specifies the necessary geometry and volume of the disinfection zone.

#### 4.3 Microorganism Susceptibility Factor for Low-UVC Exposure [\[back to TOC\]](#)

Germicidal low-UVC light has been used to disinfect and kill germs in critical healthcare and infrastructure applications for over 100 years. Researchers have determined the low-UVC dose-response relationship to inactivate or kill various viruses, bacteria, and other microorganisms. Assuming first-order rate constant and kinetics,<sup>135</sup> microorganism susceptibility to low-UVC is characterized by the single stage decay equation:<sup>136</sup>

$$C(t) = C_0 \cdot e^{-Kd}$$

where  $C(t)$  is the concentration of active microorganisms surviving after low-UVC exposure,  $C_0$  is the concentration of active microorganisms prior to low-UVC exposure,  $K$  is the microorganism susceptibility factor ( $\text{cm}^2/\text{mJ}$ ), and  $d$  is the delivered low-UVC dose ( $\text{mJ}/\text{cm}^2$ ).<sup>137</sup> Hence,

$$K_{UVC} = - (1/d_{UVC}) \cdot \ln[C(t)/C_0] \quad [\text{Eq. 34}]$$

The following studies, summarized in Table 7 with sample medium, associated shielding levels, calculated  $K_{UVC}$ , and  $d_{UVC}$  needed for 3-log inactivation, have specifically characterized low-UVC inactivation of single-strand (ss) and double-strand (ds) RNA/DNA viruses including SARS-CoV-2:

- LUV Systems (2021; unpublished)<sup>138</sup> achieved 3-log inactivation at  $d_{UVC} = 4\text{--}7$   $\text{mJ}/\text{cm}^2$  for single-strand RNA (ssRNA) virus SARS-CoV-2. Test conditions included Osram/Sylvania 254 nm light source, **the halō** Model 5R/M light fixture, and thin-film surface samples on passivated stainless steel, sealed granite, and PVC-coated fabric substrates).

**Table 7. Summary of 254 nm low-UVC inactivation studies with RNA/DNA virions.**

Research Study	Sample Medium/ Shielding Level	$K_{254}$ $\text{cm}^2/\text{mJ}$	$d_{UVC}$ (99.9% inactivation) * $\text{mJ}/\text{cm}^2$	Single- or double strand, virus
Tseng (2007-1)	Aerosol/Low	4.4-5.6	1.4	ss: MS2, phi X174
Tseng (2007-1)	Aerosol/Low	3.1	2.2	ds: Phi 6, T7
McDevitt (2012)	Aerosol/Low	2.6	2.7	ss: Influenza A, H1N1
Griffiths (2020)	Petri dish, film/Medium	1.4-2.3	3.8	ss: SARS-CoV-2
LUV Systems (2021)	Surfaces, film/Medium	0.98-1.7	5.3	ss: SARS-CoV-2
Tseng (2007-2)	Agar gelatin/Medium	0.99-1.4	5.9	ss: MS2, phi X174
Tseng (2007-2)	Agar gelatin/Medium	0.38-0.46	17	ds: Phi 6, T7
Duan (2003)	Well plate (0.3 cm)/High	0.028 **	250	ss: SARS-CoV
Darnell (2004)	Well plate (1 cm)/High	0.0042	1,600	ss: SARS-CoV

\* Where a range is provided for  $K_{254}$ , the geometric mean is used to calculate  $d_{UVC}$ .

\*\* Light source at 260 nm.

<sup>135</sup> <https://www.ncbi.nlm.nih.gov/pmc/articles/PMC7176239/#?po=17.0588>

<sup>136</sup> For alternate kinetics including two stage and shoulder curves, see: <https://www.ncbi.nlm.nih.gov/pmc/articles/PMC7176239/#?po=17.0588>

<sup>137</sup> Dose equals the intensity of the low-UVC light source upon the pathogen sample multiplied by exposure time.

<sup>138</sup> <https://www.tinyurl.com/LUVsystems18>

- Griffiths (2020)<sup>139</sup> achieved 3-log inactivation at  $d = 3\text{-}5 \text{ mJ/cm}^2$  for ssRNA virus SARS-CoV-2. Test conditions included Signify/Philips 254 nm light source, and thin-film surface samples in Petri dishes (wet/dry).
- McDevitt (2012)<sup>140</sup> achieved ~1.7-log inactivation at  $d = 1.5 \text{ mJ/cm}^2$  for ssRNA influenza A virus H1N1. Test conditions included Lumalier 254 nm light source, **aerosol** samples in an exposure chamber, and 25-50% RH. This research also considered RH at 75% and found the low-UVC inactivation efficacy to decrease with increased humidity.
- Tseng (2007-1)<sup>141</sup> achieved 2.3-log inactivation at  $d = 0.95\text{-}1.2 \text{ mJ/cm}^2$  for ssRNA/DNA viruses MS2 and phi-X174. For dsRNA/DNA virions phi 6 and T7,  $1.2 \text{ mJ/cm}^2$  provided ~1.6 log inactivation. Test conditions included Philips 254 nm light source, viral samples **aerosolized** in an exposure chamber, and 55% RH. This research also included the same trials at 85% RH, and the microorganism susceptibility factor, K, was 25-50% less at the higher humidity level.
- Tseng (2007-2)<sup>142</sup> achieved 3-log inactivation at  $d = 5\text{-}7 \text{ mJ/cm}^2$  for ssRNA/DNA viruses MS2 and phi-X174, and 15-18  $\text{mJ/cm}^2$  ( $K = 0.00038\text{-}0.00046 \text{ cm}^2/\text{mJ}$ ) for double-strand (ds) RNA/DNA viruses phi 6 and T7. Test conditions included Philips 254 nm light source, thin-film surface samples on a gel-agar matrix, and 55% RH.
- Darnell (2004)<sup>143</sup> achieved 2.6-log inactivation at  $d = 1,440 \text{ mJ/cm}^2$  for ssRNA virus SARS-CoV. Test conditions included a Spectronics 254 nm low-UVC light source, and well plate samples in 1-cm depth aliquot suspensions.
- Duan (2003)<sup>144</sup> achieved almost complete inactivation<sup>145</sup> at  $d = 162 \text{ mJ/cm}^2$  for ssRNA virus SARS-CoV. Test conditions included an unspecified 260 nm low-UVC light source, and well plate samples in 0.3 cm depth aliquot suspensions.

Figure 13 depicts these results in terms of required low-UVC dose  $d_{\text{UVC}}$  needed for 99.9% virus inactivation. Four key observations from the research data:

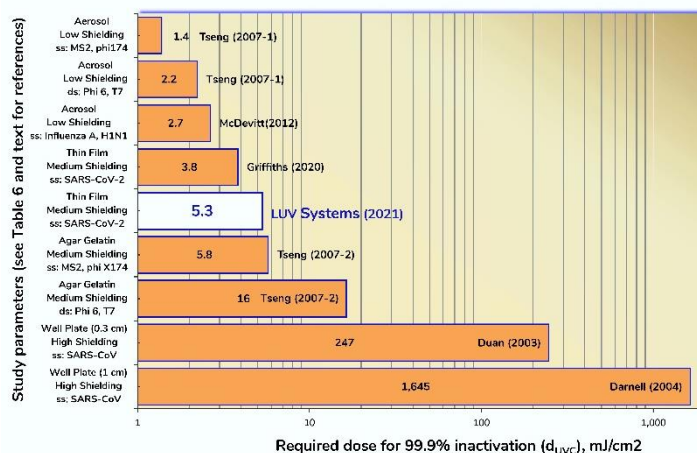
1. Single-strand RNA/DNA viruses are 3-5x more susceptible to low-UVC inactivation than double-strand viruses.
2. Virions contained in aqueous suspension are less susceptible to low-UVC inactivation in comparison to unshielded virions, say in a thin-film on a surface or in aerosol form.
3. Increased RH decreases the low-UVC susceptibility of virions in aerosols.
4. Aerosolized virions are 4x+ more susceptible to low-UVC inactivation than on surfaces.

These findings provide a design basis for **the halō** and associated proprietary dose-inactivation algorithm for pathogen-containing aerosols. Airborne PPQ are more susceptible to low-UVC because of increasingly less shielding as moisture evaporates, a lack of surface imperfections or liquid phase that can otherwise provide shielding, multiple passes of reflected light across the exposure volume, and unconstrained rotational momentum. Along with volumetric air flow specifications discussed earlier, these dose-response data provide optimal exposure dose and residence time in **the halō** disinfection zone to inactivate pathogens.

#### 4.4 Minimize Mixing of Treated and Untreated Air [\[back to TOC\]](#)

Unlike flow in pipes or ducts, air in a room follows unconstrained, or open channel, steady-state flow lines. If there is mixing due to the orientation of HVAC and ventilation vents, NDOs such as open windows, physical obstacles that impede linear flow lines, significant temperature gradients that create thermal convective flows, or significant movement of people or objects, the air in the breathing zone becomes mixed with the rest of the air in a room. Airborne pathogens will then mix throughout the volume of the

Figure 13. Low-UVC dose needed for 99.9% virus inactivation (semilog).



<sup>139</sup> <https://www.researchsquare.com/article/rs-65742/v1>

<sup>140</sup> <https://aem.asm.org/content/78/6/1666>

<sup>141</sup> <https://www.tandfonline.com/doi/full/10.1080/02786820500428575>

<sup>142</sup> <https://www.ncbi.nlm.nih.gov/pmc/articles/PMC7196698/>

<sup>143</sup> <https://www.ncbi.nlm.nih.gov/pmc/articles/PMC7112912/>

<sup>144</sup> [www.tinyurl.com/LUVsystems19](http://www.tinyurl.com/LUVsystems19)

<sup>145</sup> Assumed 2-log reduction.

room. HVAC systems, downflow ceiling fans, and other air moving devices are not designed to minimize this mixing, hence they create a respiratory infection risk for everyone in the room.

As opposed to a continuously stirred condition, it is possible to mimic unmixed, pipe-like plug flow in open channels if the air is pulled rather than pushed by a fan. With **the halō's** upflow fan, this condition is approached by segregating potentially infectious breathing zone from treated air returning from **the halō**. **the halō** draws air up from the breathing zone, directs it into the encapsulated light ring disinfection zone, and then pushes the treated air back into the breathing zone away from the fan's intake. Hence there is no short-circuiting of treated air or mixing with untreated air. The flow lines created by this configuration exhibit steady-state laminar characteristics and may result in resonant standing waves. With **the halō's** proprietary modulation algorithm, resonance is eliminated without disturbing the laminar flow regime.



#### 4.5 Impact on HVAC Systems [\[back to TOC\]](#)

HVAC systems may have return and supply points at or in the ceiling, in walls, or in the floor. Return and supply are separated by distance to allow good mixing of conditioned air through a room. Depending on the location of the various registers, airflow circuits develop through the room volume, including mixing, eddies, and turbulence zones. While **the halō** does not eliminate these disturbances to optimal laminar flow, it does provide control of the breathing zone so that mixing of untreated air is substantially reduced or eliminated. In any circumstance, **the halō** works in conjunction with HVAC systems and improves airflow to reduce detrimental mixing of treated and untreated air, and most importantly, to disperse/break up respiratory jets from potentially infected sources.

#### 4.6 Comparative Energy Burden and Carbon Footprint [\[back to TOC\]](#)

**the halō** is rated at 650 W, so with 12 hr/day, 6 day/wk operation, the annual energy consumption is 2,400 kWh – at the prevailing electricity rate in California around \$0.20/kWh, the annual energy cost is around \$480 to achieve over 30 ACH<sub>e</sub>. For a comparison to ventilation-based ACH alternatives, two scenarios are considered – a baseline with 2.8 ACH, and projection at 12 ACH, the minimum standard for high respiratory infection risk environments, such as operating rooms.





Table 8. Energy burden and carbon footprint at 2.8 and 12 ACH (annualized per classroom, excludes capital costs; rounded).

Location	@ 2.8 ACH (450 CFM outside air, baseline)				@ 12 ACH (1,940 CFM outside air)			
	Electricity kWh	Natural Gas therms	Energy Cost US\$	CO <sub>2</sub> Emissions metric tons	Electricity kWh	Natural Gas therms	Energy Cost US\$	CO <sub>2</sub> Emissions metric tons
Boston, MA	1,900	150	590	2.2	8,300	660	2,500	9.4
Chicago, IL	2,300	180	420	2.6	9,900	790	1,800	11
Houston, TX	6,500	23	860	4.7	28,000	99	3,700	20
Los Angeles, CA	2,500	4.2	470	1.8	11,000	18	2,000	7.8
Miami, FL	8,700	0.81	940	6.2	38,000	3.5	4,100	27

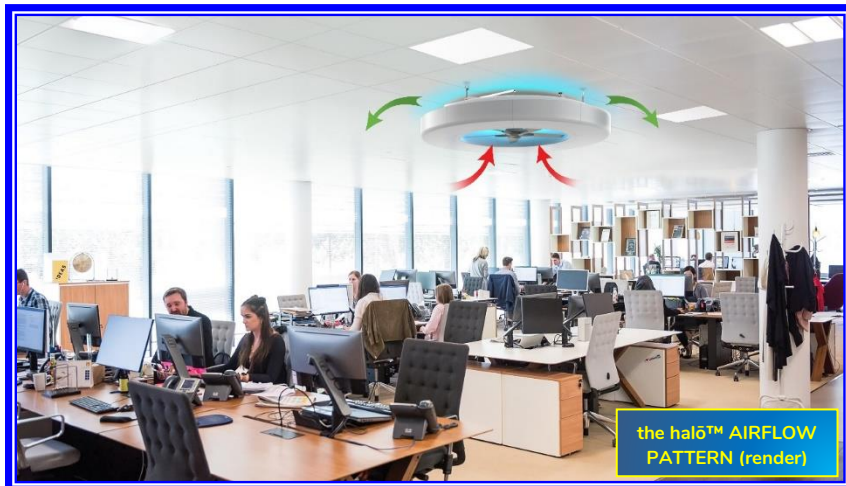
Specifically pertaining to operating rooms and hospital-acquired infections, Gormley<sup>146</sup> studied three operating rooms, averaging 560 ft<sup>2</sup> each. Increased energy costs for HVAC fans, pumps, cooling, heating, humidification, and steam at projected at \$1,466/ACH/yr per operating room. For an increase from 2.8 ACH to 12 ACH, and extrapolating to 1,000 ft<sup>2</sup> rooms with 0.6 scaling exponent, this represents an excess energy cost over \$19,000/yr per operating room and associated excess CO<sub>2</sub> emissions.

Another resource, enVerid,<sup>147</sup> provides a spreadsheet-based energy estimator<sup>148</sup> for HVAC-based ventilation strategies to increase ACH. The following model inputs were used to estimate excess energy burden/carbon footprint for increasing ACH in a classroom:

- Classroom for age 9 plus, 30 occupants;
- 1,000 ft<sup>2</sup> floor area, 9.7 ft ceiling height;
- Total supply airflow = outside airflow (neglecting non-ventilation air circulation);
- No filtration or treatment, only ventilation;
- Cooling by electricity, and heating with natural gas;
- Operation 12 hours/day, 6 days/week;
- 450 CFM outside air for 2.8 ACH base case;
- 1,940 CFM outside air for 12 ACH scenario; and,
- City-specific utility rates from spreadsheet.

Table 8 provides a summary at 2.8 ACH and 12 ACH, with excess annual energy use, energy cost, and carbon footprint (CO<sub>2</sub> emissions) estimated by the model for various US cities. The 12 ACH scenario increases energy cost by \$1,400-\$3,100/yr and contributes 6 to 21 metric tons of excess CO<sub>2</sub> emissions. This assessment excludes equipment upgrade, maintenance, and replacement costs for running the HVAC at high ACH continuously while people are present.

As seen with the Honeywell HPA 300 purifiers, increasing ACH via increased ventilation/HVAC does not ensure reduced risk of respiratory infection, particularly for short-term exposures. Traditional HVAC/ventilation systems do not disperse respiratory jets, control the breathing zone, or provide directional airflow, even with high ACH rates. ACH can increase the PPQ depletion rate over the long-term, but short-term localized exposures are not necessarily mitigated.



<sup>146</sup> <https://www.onsite-llc.com/s/Cost-benefit-analysis-of-different-air-change-rates-in-an-operating.pdf>

<sup>147</sup> <https://enverid.com/blog/the-enverid-covid-19-energy-estimator-revealing-the-full-costs-of-hvac-strategies/>

<sup>148</sup> <https://drive.google.com/file/d/17H69NUZGiyo0BhCdId0dR4TVQ3YoPW53/view>



## 5 Conclusions [\[back to TOC\]](#)



- While environmental agencies regulate excess cancer risk to below 100 in one million over 70 years of exposure, to date the United States has seen close to 3,000 COVID-19 deaths and over 240,000 infections per million population. In spite of this, no environmental or public health agency has established health risk-based IAQ regulatory standards for pathogen exposure in public, non-health care areas.
- The unified infectious dose model predicts and quantifies benefits and limitations of respiratory transmission mitigation measures including face coverings, social distancing, partitions, ventilation, and treatment/filtration of indoor air. Results are as expected based on common-sense principles.
- Masks/ partitions are effective at dispersing respiratory jets and localized PPQ concentrations for exposures < 1-2 hr.
- Social distancing is effective at preventing short-term < 30 min exposure to high PPQ loading in localized respiratory jets.
- For long-term exposures > 1 hr, ventilation and treatment/filtration are critical to mitigate the risk of respiratory transmission (maximizing  $\beta$  or the PPQ depletion rate).
- The model can generate probabilistic risk scores for indoor air and guide respiratory transmission mitigation strategies - predictions are within 13% of the CDC's 15-min guidance for potential COVID-19 exposure.
- Without proper consideration of nonhomogeneous PPQ concentrations in localized regions within the breathing zone, such as proximal or downwind of an infected source, the risk of infection may be underestimated by > 20x.
- For short-term exposures, dispersal/breaking up the respiratory jet is critical to mitigate respiratory transmission.
- Any means to isolate potentially infectious air in the breathing air, including vertical air movement and minimizing mixing of treated and untreated air, is critical in mitigating the risk of respiratory transmission.
- Running a simple ceiling fan, preferably in reverse or upflow mode, can provide limited short-term protection from respiratory infection.
- A new metric, the APMI, is proposed as a practical and actionable health-based index to inform and guide facility managers and the public with respect to respiratory infection risk. APMI results are mostly consistent with the less versatile risk parameter proposed by Peng (2022), although infectious pathogen quanta generation rates are significantly different.
- the halō is a practical and effective means to disinfect indoor air continuously, while people are present:
  - With an active source, the halo is 10x+ better than any disinfection alternative, 3x better than social distancing and masks for all receptors, and 30x better than the no mitigation base case.
  - With an initial airborne PPQ level but no continuing source, the halo clears pathogens >4x faster than the no mitigation base case and >2x faster than any other mitigation option.
- the halō provides over 30 ACH<sub>e</sub> with 20% of a room's air treated/min and effective breathing zone control. This is over 2x the CDC/ASHRAE minimum 10-15 ACH requirement for critical health care locations such as surgical wards.

- For rooms with a high concern of infection, such as operating rooms, the annual energy cost of increased ventilation for 12 ACH may be over \$19,000 with a corresponding increase in excess CO<sub>2</sub> emissions.
- HVAC-based ventilation can be increased to provide higher ACH, but requires much more energy use, equipment modifications and maintenance, and significant excess CO<sub>2</sub> emissions. A 12 ACH increase for a classroom or other 1,000 ft<sup>2</sup> room may add \$1,400-\$3,100/yr in energy costs alone, with 6-21 metric tons of excess CO<sub>2</sub> emissions per year.
- Achieving 12 ACH via ventilation or portable air purifiers may reduce the long-term PPQ loading, but short-term respiratory infection risk is mitigated by dispersing respiratory jets, controlling the breathing zone, and providing directional airflow.
- For comparison, **the halō** is rated at 650 W, so with 12 hr/day, 6 day/wk operation, the annual energy consumption is 2,400 kWh. Based on California energy rates, this corresponds to \$480/yr to achieve over 30 ACH<sub>e</sub>, while concurrently dispersing respiratory jets, controlling the breathing zone, and providing directional airflow.

